

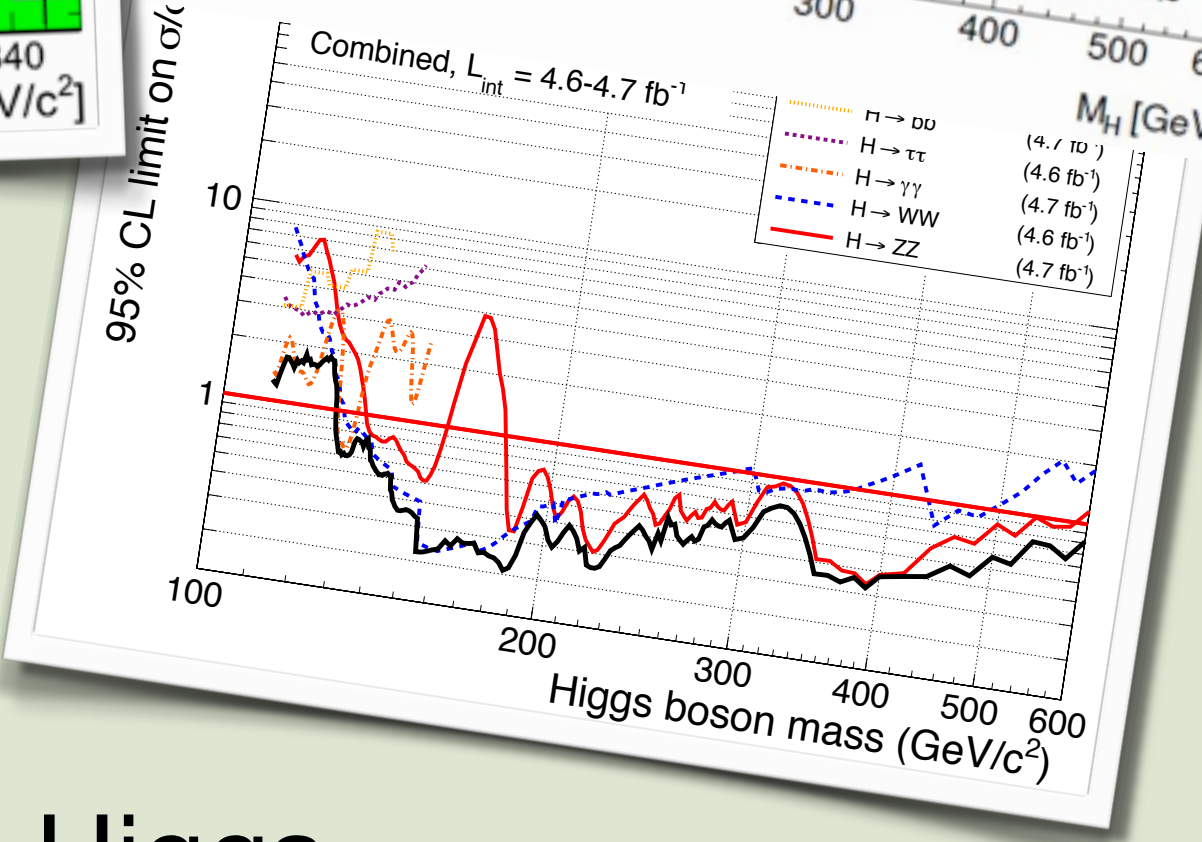
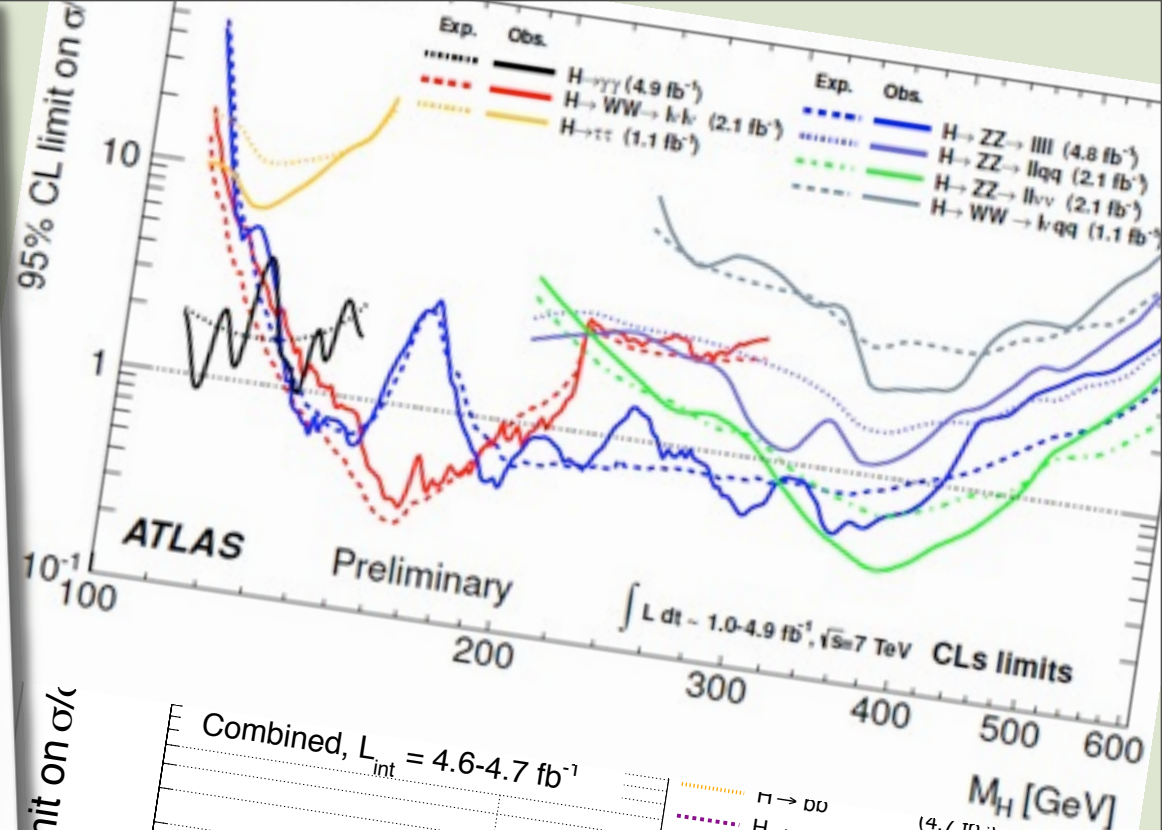
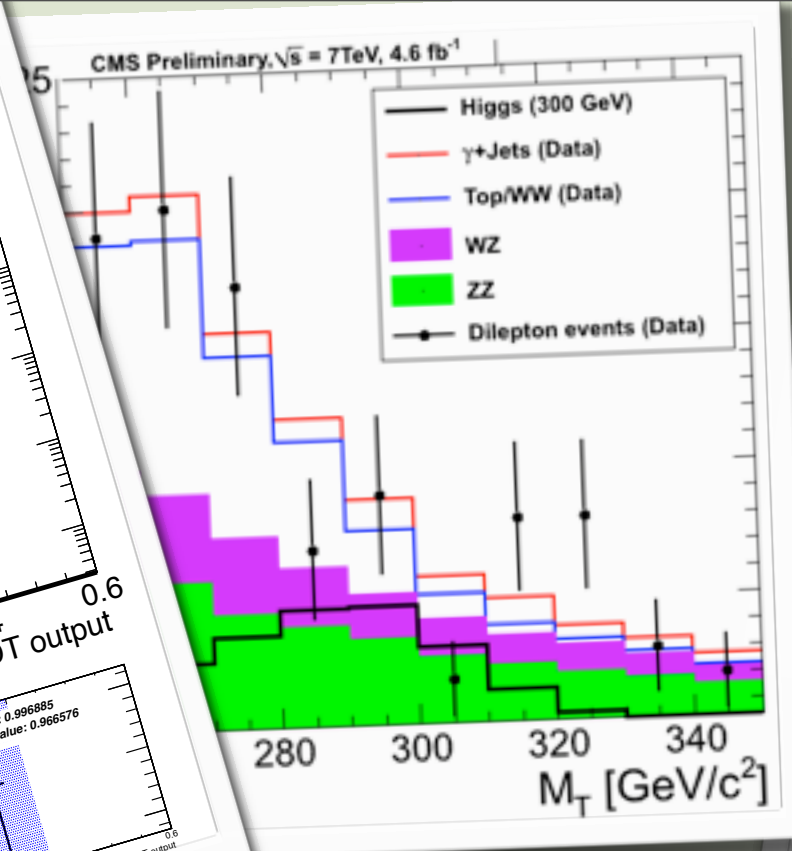
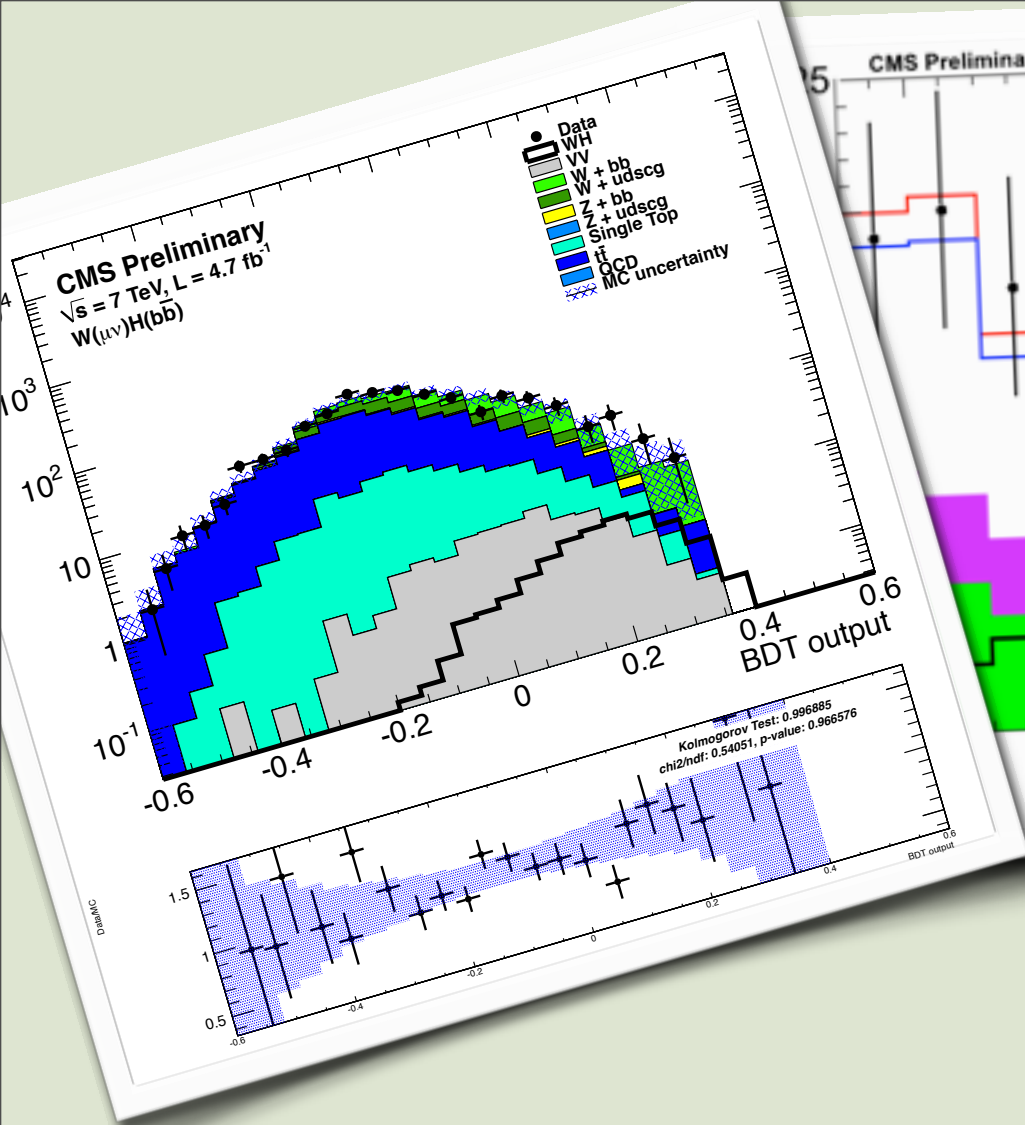
Fully differential NNLO cross-sections for Higgs boson production

Achilleas Lazopoulos

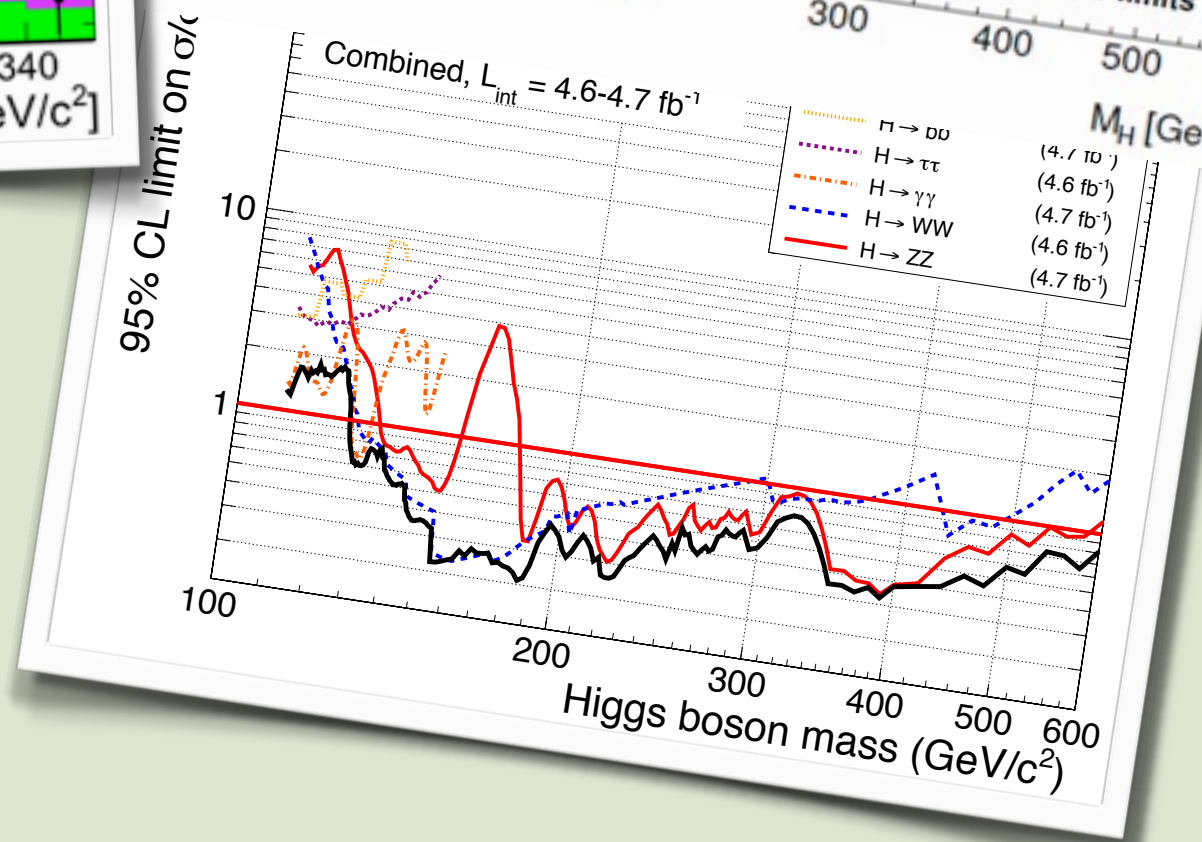
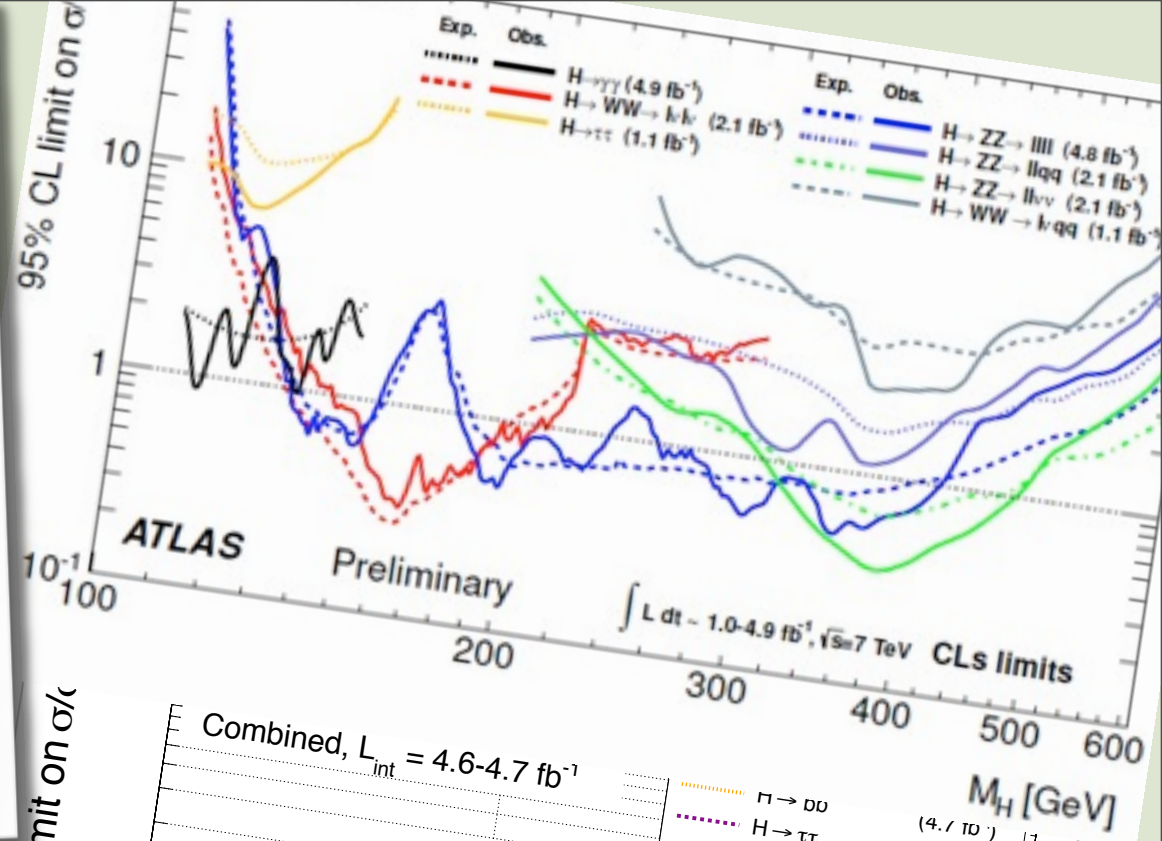
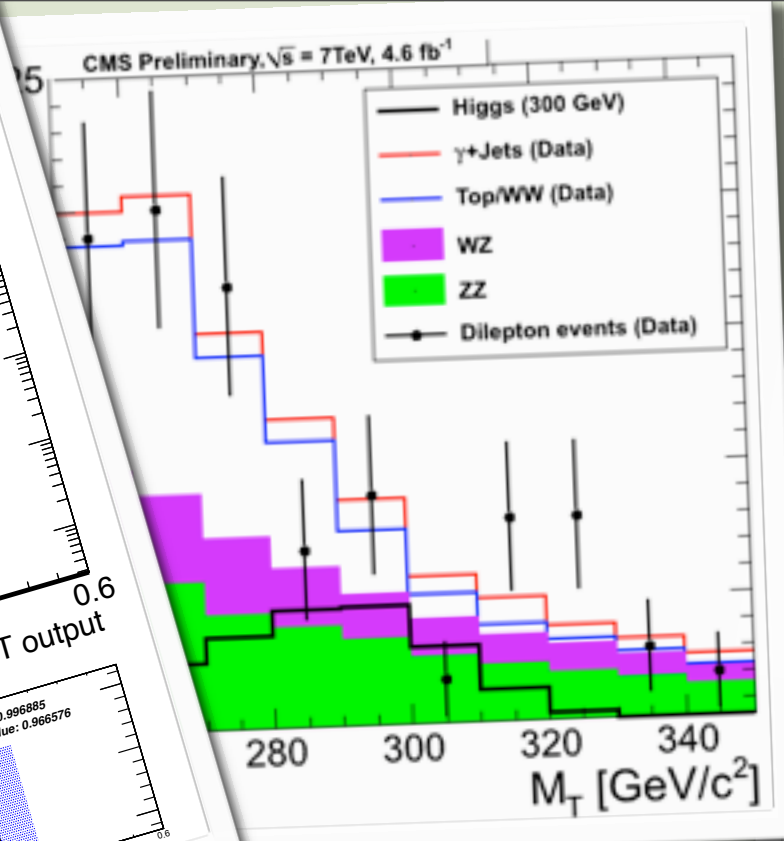
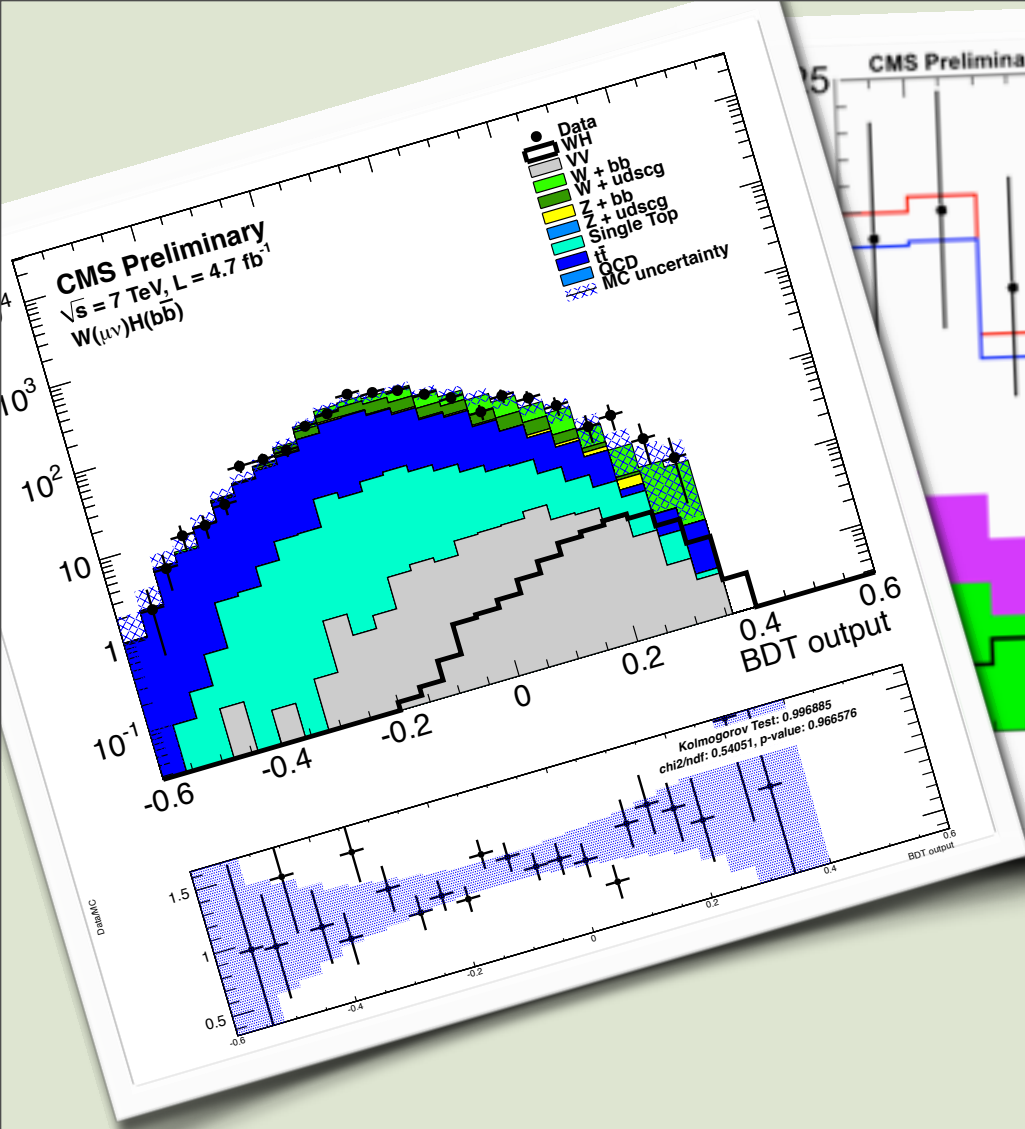
ETH Zurich

ZPW2012: 'Higgs search confronts theory'

work in collaboration with A. Aeberli, C. Anastasiou, S.
Buehler, F. Dulat, F. Herzog, B. Mistlberger, R. Mueller



To find the Higgs
 very sophisticated searches are employed



They depend on predictions of production rates & on fine details in kinematic distributions.

How is the number of Higgs events estimated ?

Overall normalization from very precise inclusive cross section rates.

How is the number of Higgs events estimated ?

Overall normalization from very precise inclusive cross section rates.

Kinematic distributions from parton shower MC (with LO, LL or NLO accuracy).

Pythia, Herwig, MC@NLO,
POWHEG, Alpgen, Sherpa

How is the number of Higgs events estimated ?

Pythia, Herwig, MC@NLO,
POWHEG, Alpgen, Sherpa

Overall normalization from very precise inclusive cross section rates.

Kinematic distributions from parton shower MC (with LO, LL or NLO accuracy).

Differential distributions from more precise calculations to control MC or to compare directly with binned data.

How well do we understand the kinematic distributions

of the Higgs boson

of its decay products

of associated radiation



Pretty well in general, but there is room for improvement.

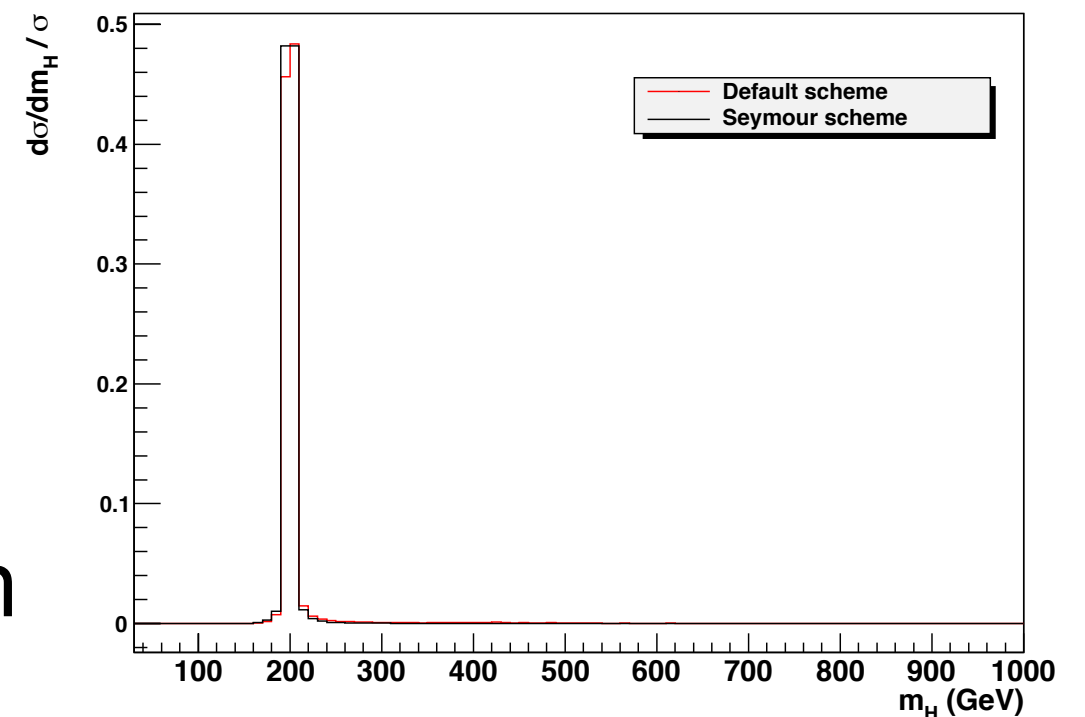
Even for the simplest of distributions:

The invariant mass distribution of the Higgs boson



If the Higgs is **light**

then it's also **thin**:
an uneventful spike well thinner
than the experimental resolution





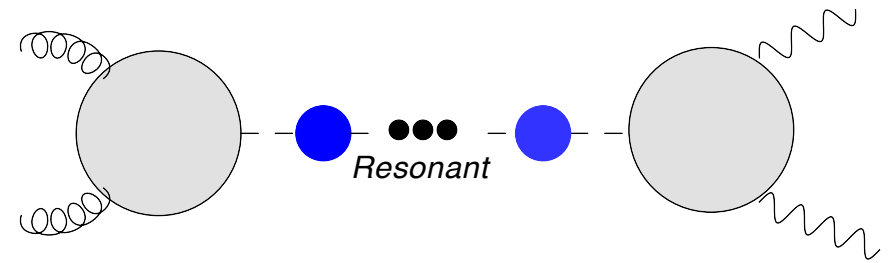
But if the Higgs is **heavy** ($>500\text{GeV}$)

which is **not** excluded experimentally

It could be part of a sensible but more complicated Higgs sector (2HDM, Susy, etc.)

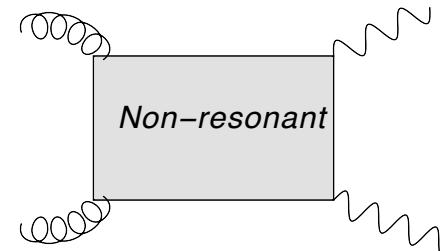
then it's also **wide!**

$$\mathcal{A} = \mathcal{A}_{gg \rightarrow H}(Q) \frac{i}{Q^2 - M_h^2 + \Sigma(Q^2)} \mathcal{A}_{H \rightarrow VV}$$



+ $\mathcal{A}_{\text{rest}}$

+



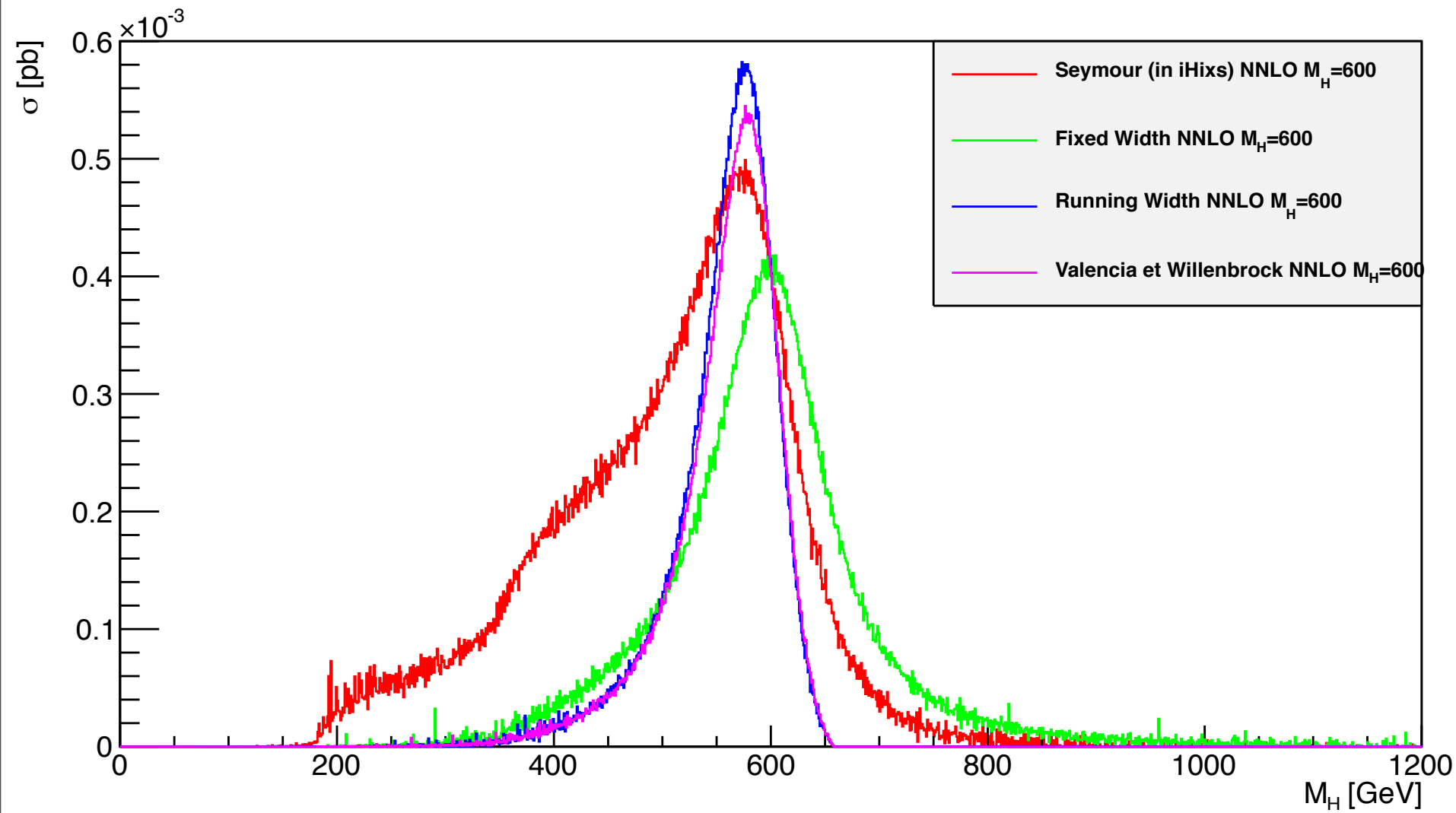
Amplitudes to produce a final state from a not-so-narrow Higgs boson require decay widths at the virtuality, Q , not the Higgs mass.

$$\mathcal{A} \sim \sqrt{\Gamma_{gg \rightarrow H}(Q)} \frac{iZ(Q)}{Q^2 - M_{phys}^2 + iZ(Q)\Gamma(Q^2)} \sqrt{\Gamma_{H \rightarrow VV}(Q)} + \mathcal{A}_{\text{rest}}$$

$$\mathcal{A} \sim \sqrt{\Gamma_{gg \rightarrow H}(Q)} \frac{iZ(Q)}{Q^2 - M_{phys}^2 + iZ(Q)\Gamma(Q^2)} \sqrt{\Gamma_{H \rightarrow VV}(Q)} + \mathcal{A}_{rest}$$

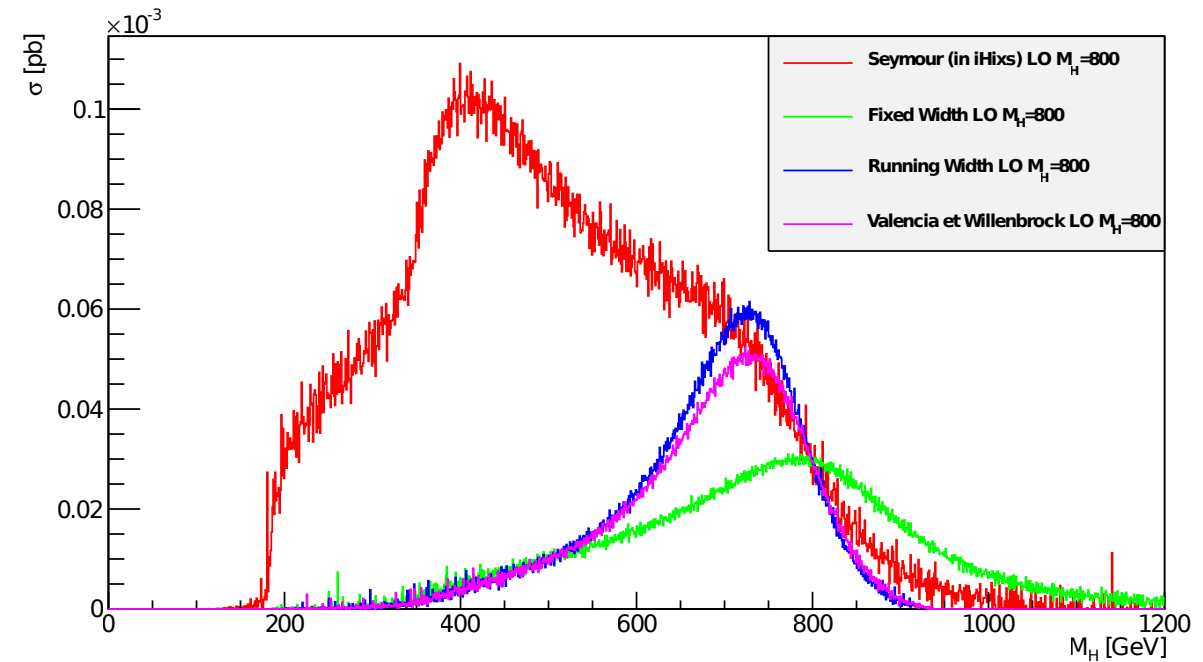
Theory predictions can be very sensitive to taking the limit $Q \sim M_h$

Invariant mass distribution

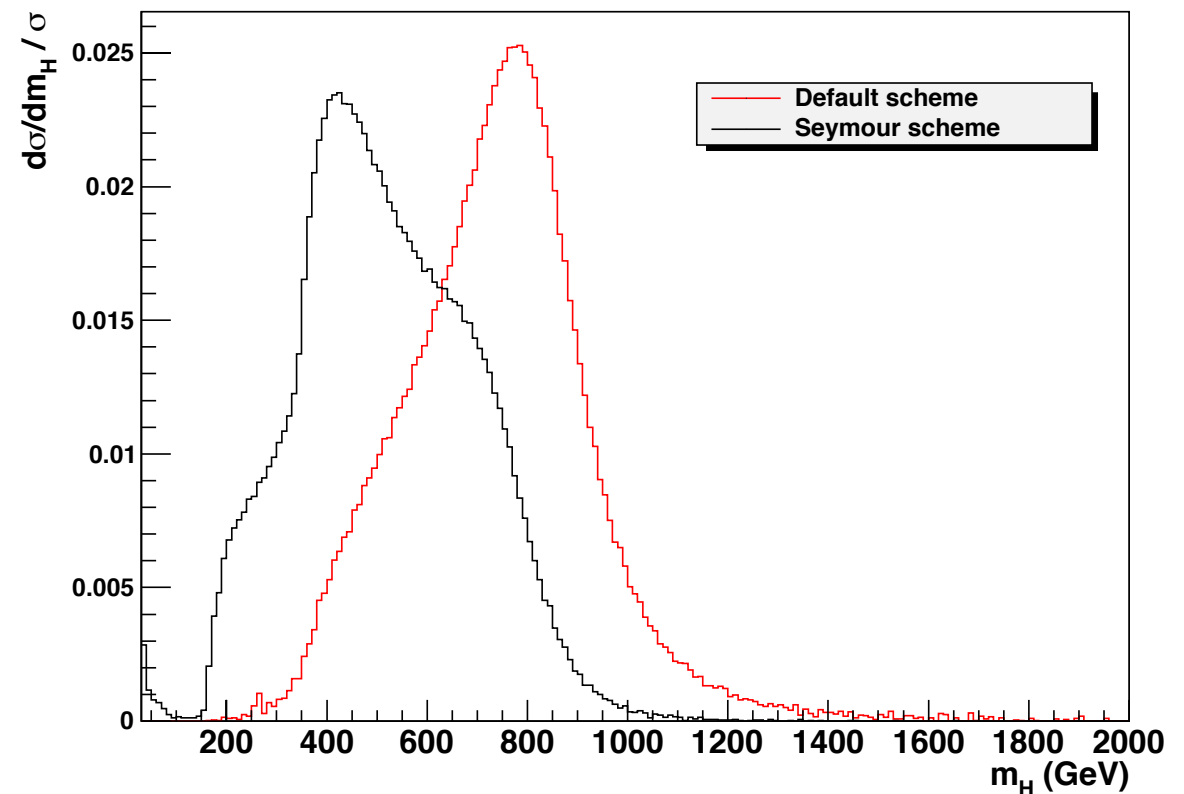
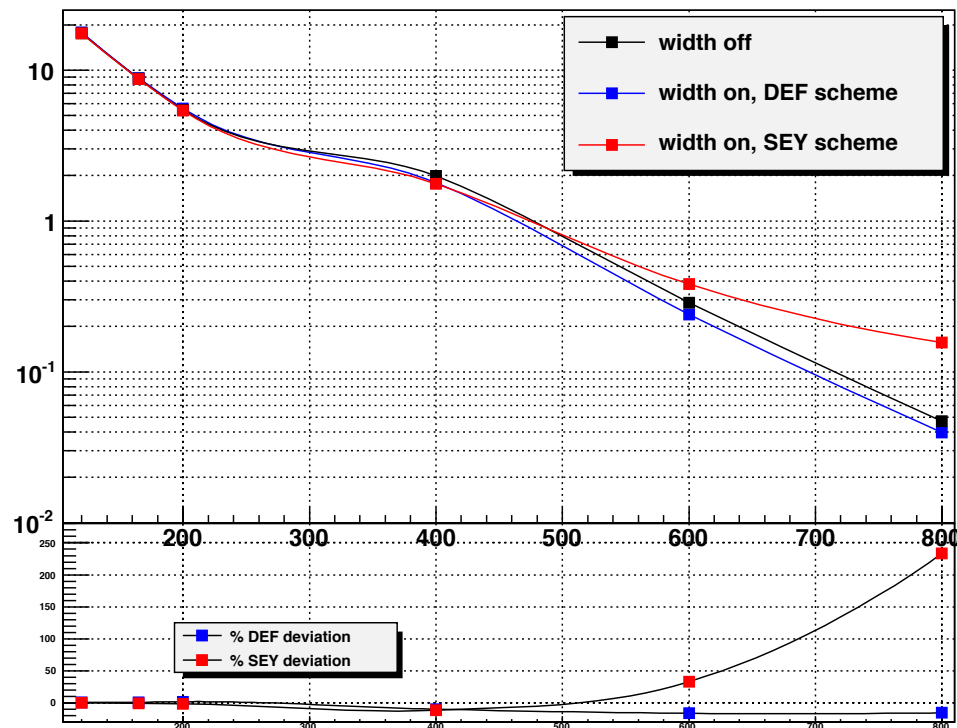


...very, very sensitive!

Invariant mass distribution



iHixs is the **only** fixed order cross-section calculation which allows for the width and branching ratios to vary with the Higgs virtuality.



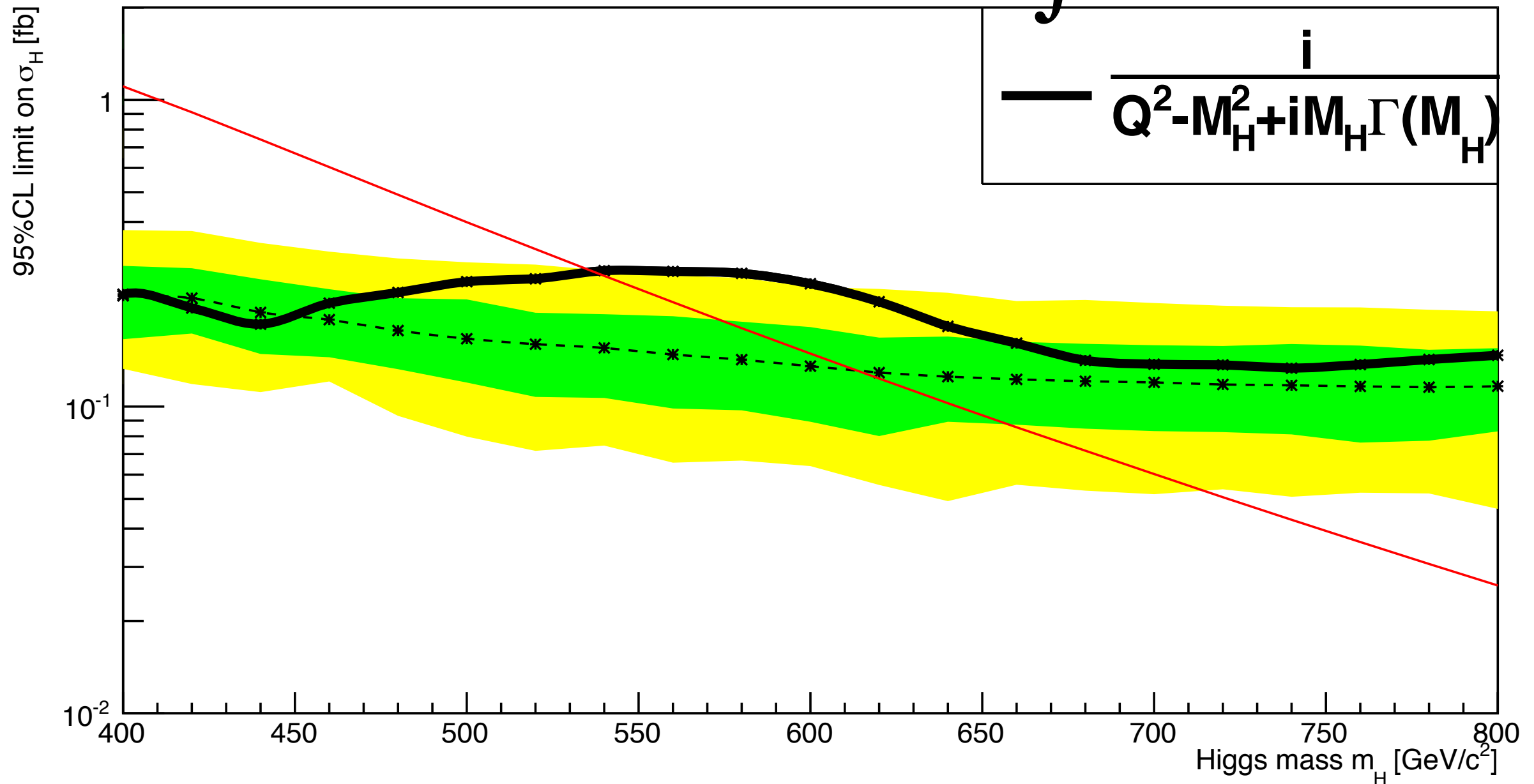
There are significant differences in the estimate of the total cross section from the approximation used in experimental studies.

Very important effects on the signal line-shape are expected also due to signal-background interference.

ATLAS and CMS start excluding very wide Higgs bosons.

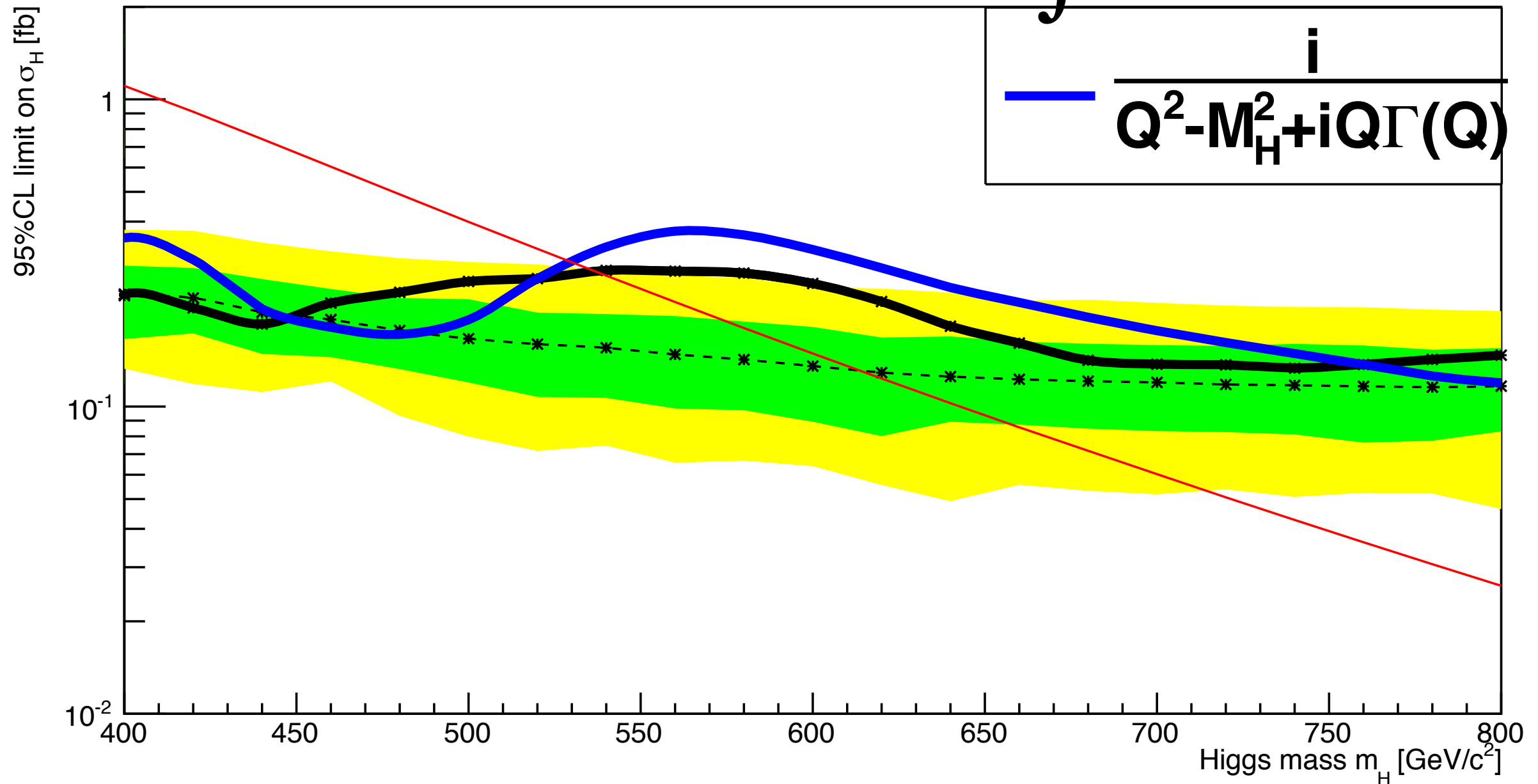
Is there an effect on exclusion limits?

600 GeV SM Higgs Exclusion Plot @ $\int L dt = 100 \text{ fb}^{-1}$



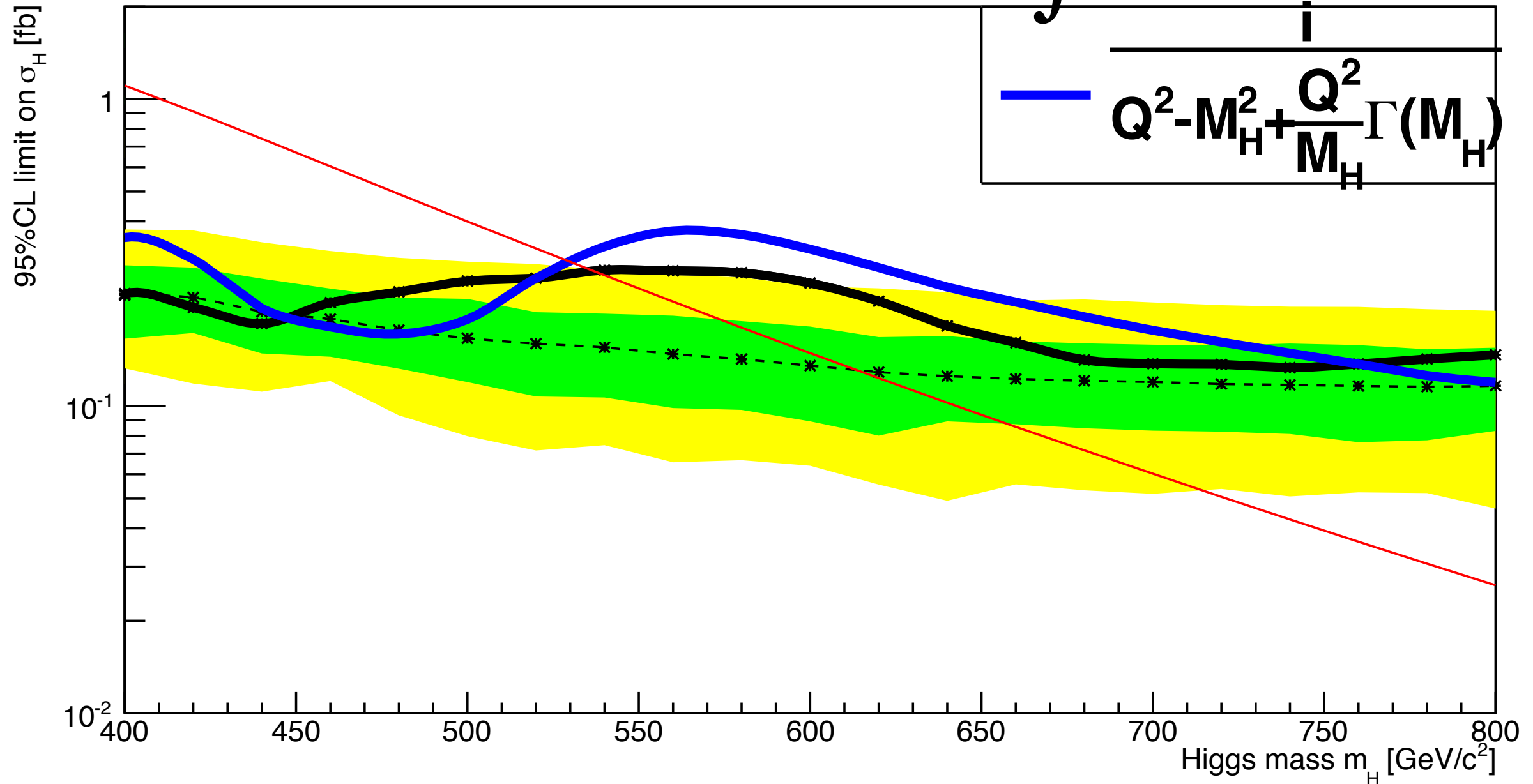
A plain Breit-Wigner as part of the signal hypothesis (black line) would lead to differences in exclusion limits than a line-shape that approximates the sum of resonant and non-resonant diagrams in gluon fusion (Seymour scheme).

600 GeV SM Higgs Exclusion Plot @ $\int L dt = 100 \text{ fb}^{-1}$



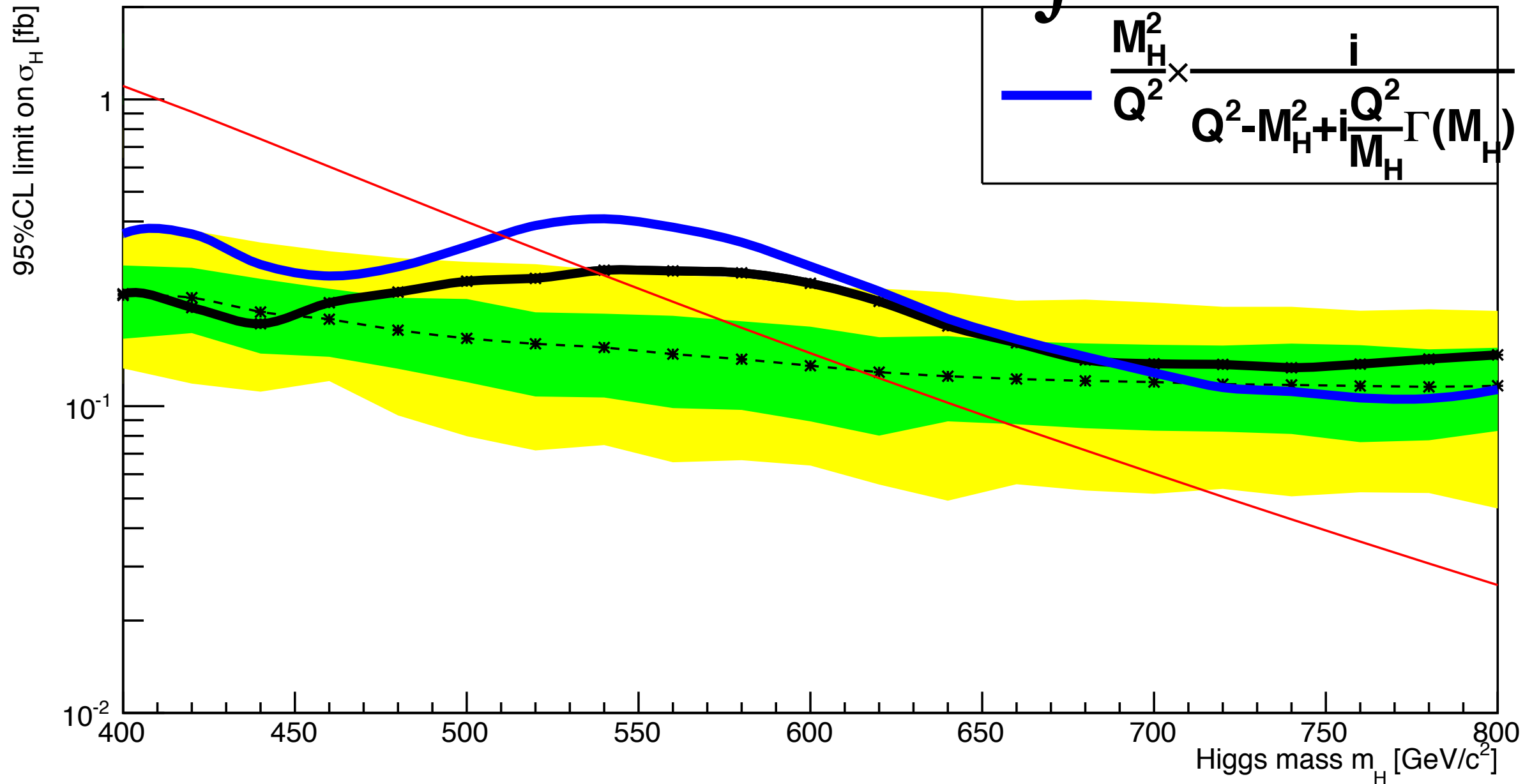
A plain Breit-Wigner as part of the signal hypothesis (black line) would lead to differences in exclusion limits than a line-shape that approximates the sum of resonant and non-resonant diagrams in gluon fusion (Seymour scheme).

600 GeV SM Higgs Exclusion Plot @ $\int L dt = 100 \text{ fb}^{-1}$



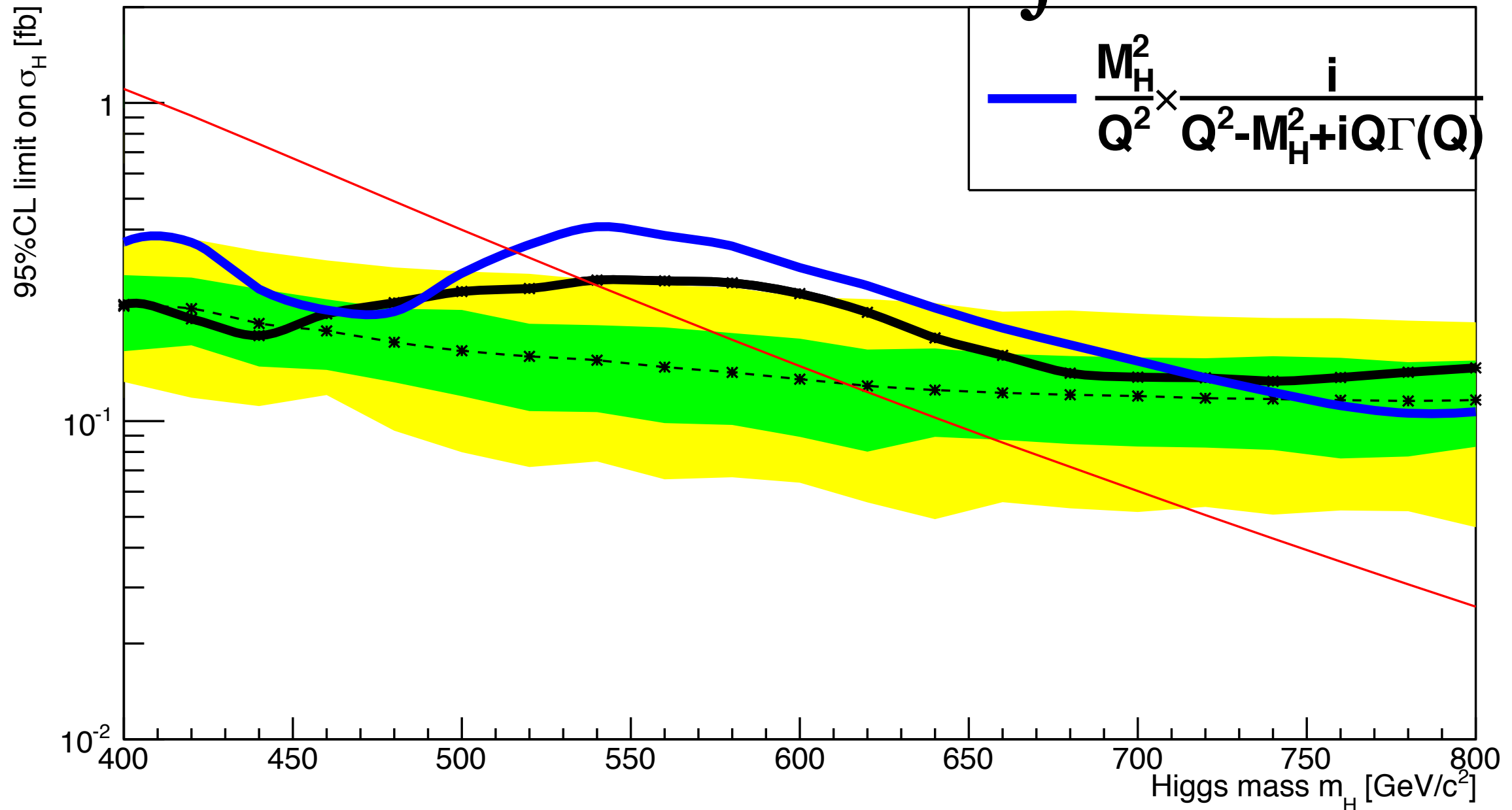
A plain Breit-Wigner as part of the signal hypothesis (black line) would lead to differences in exclusion limits than a line-shape that approximates the sum of resonant and non-resonant diagrams in gluon fusion (Seymour scheme).

600 GeV SM Higgs Exclusion Plot @ $\int L dt = 100 \text{ fb}^{-1}$



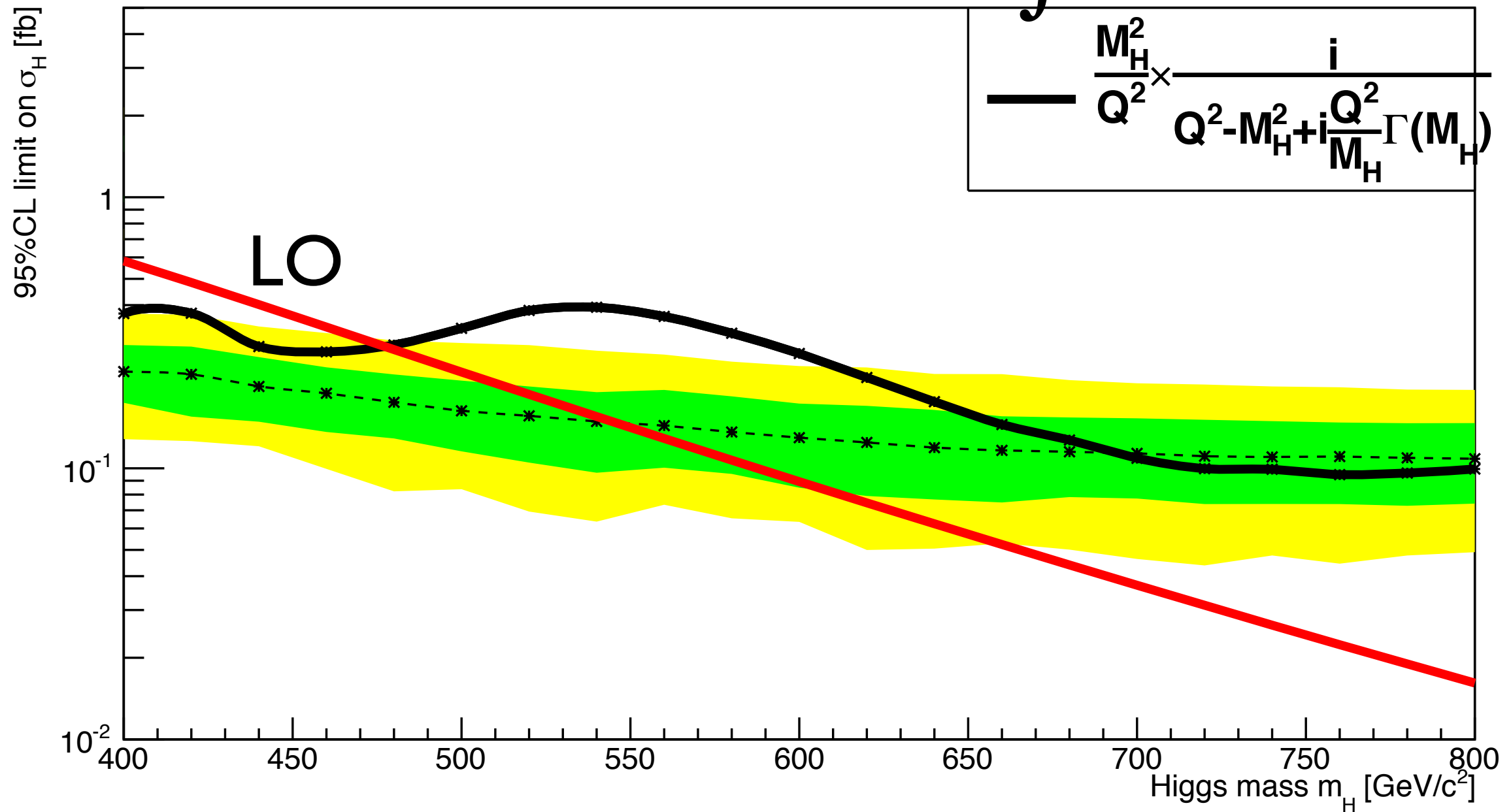
A plain Breit-Wigner as part of the signal hypothesis (black line) would lead to differences in exclusion limits than a line-shape that approximates the sum of resonant and non-resonant diagrams in gluon fusion (Seymour scheme).

600 GeV SM Higgs Exclusion Plot @ $\int L dt = 100 \text{ fb}^{-1}$



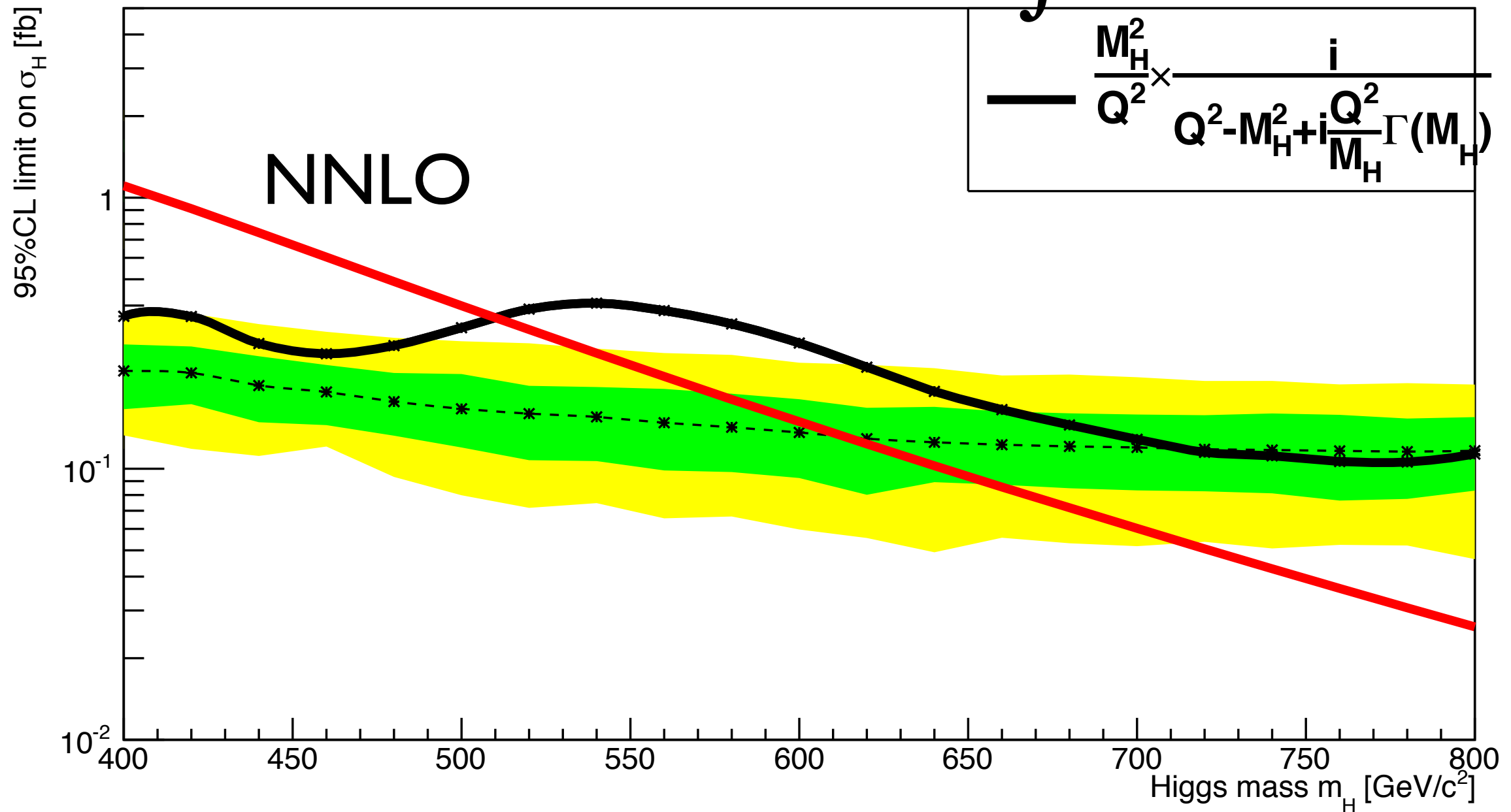
A plain Breit-Wigner as part of the signal hypothesis (black line) would lead to differences in exclusion limits than a line-shape that approximates the sum of resonant and non-resonant diagrams in gluon fusion (Seymour scheme).

600 GeV SM Higgs Exclusion Plot @ $\int L dt = 100 \text{ fb}^{-1}$



The role of the higher order corrections: realistic exclusion limits require the number of hypothetical signal events.

600 GeV SM Higgs Exclusion Plot @ $\int L dt = 100 \text{ fb}^{-1}$



The role of the higher order corrections: realistic exclusion limits require the number of hypothetical signal events.

A very heavy Higgs might be considered unviable for theoretical reasons, but care is needed before we conclude that **LHC data** disfavors or excludes such a possibility.

More complicated distributions

HQT

resumed transverse momentum distribution with the possibility to match with NNLO (Bozzi, Catani, de Florian, Grazzini 2003&2006, de Florian, Ferrera, Grazzini, Tommasini, 2011).

HNNLO

fully differential (Catani & Grazzini 2007, Grazzini 2008)

FeHiPro

fully differential but never officially released

WH production

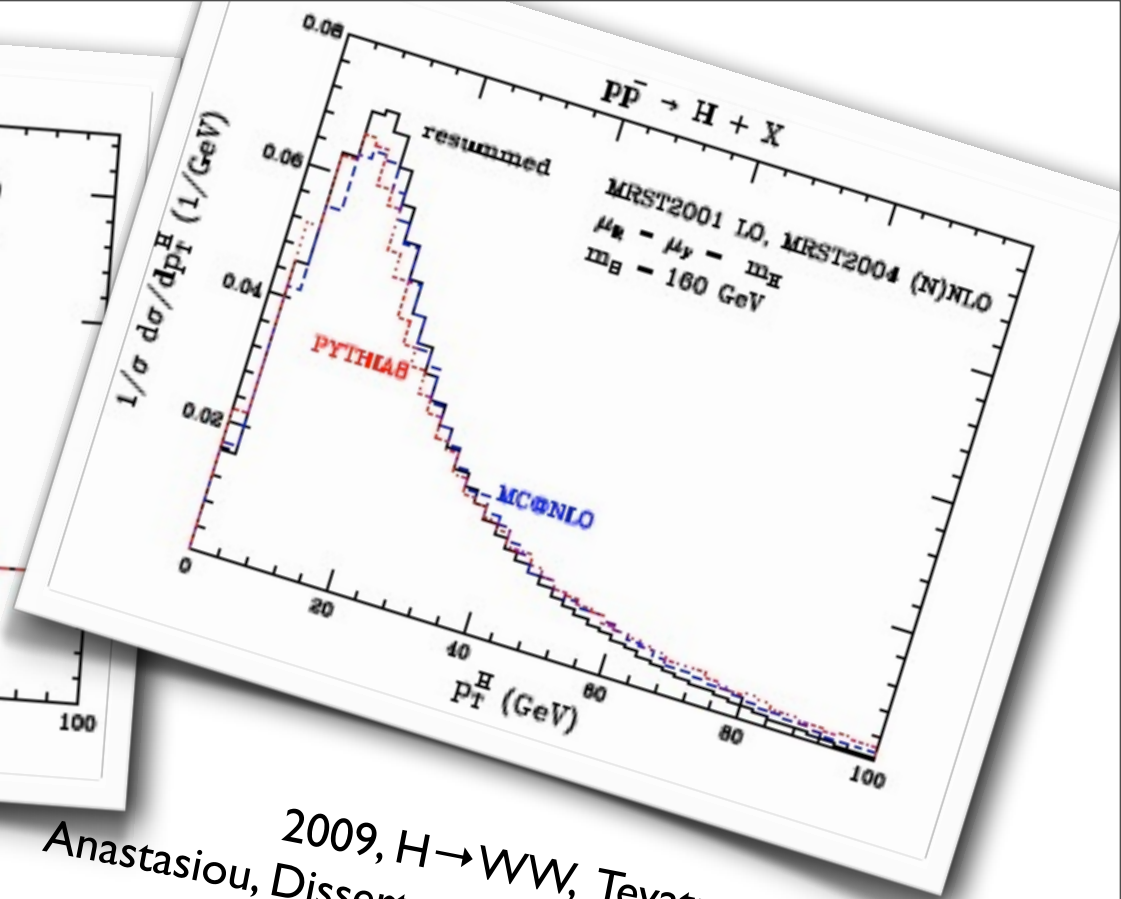
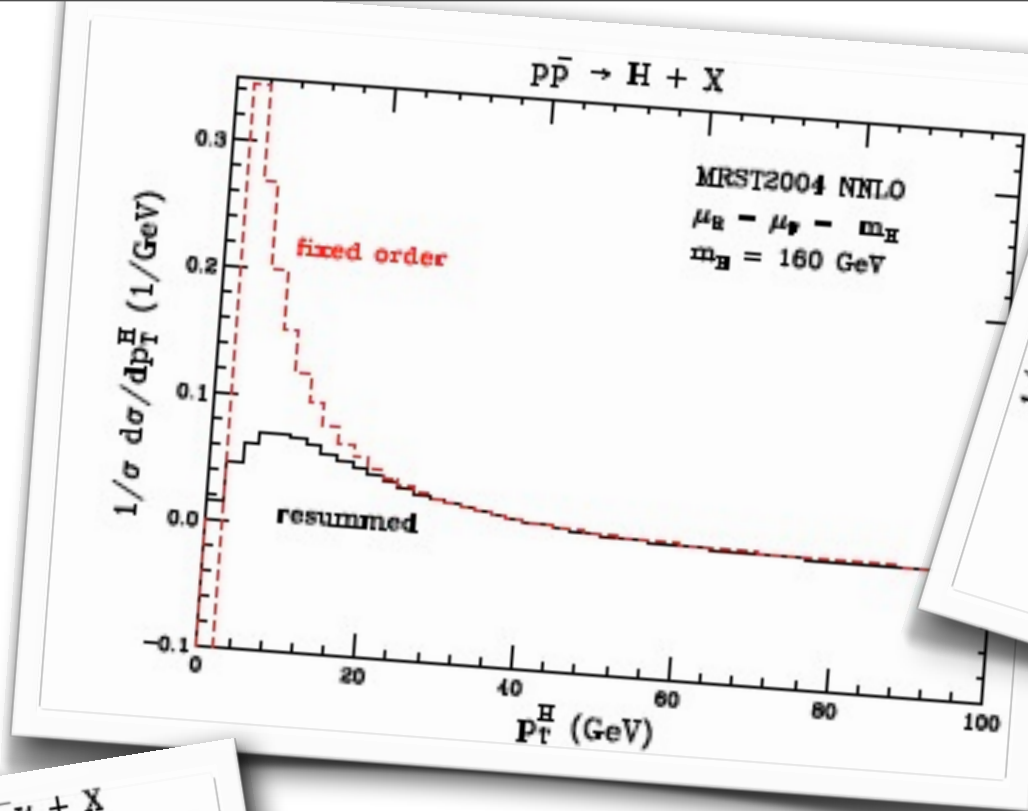
fully differential (Ferrera, Grazzini, Tramontano 2011)

$H \rightarrow b\bar{b}$ production

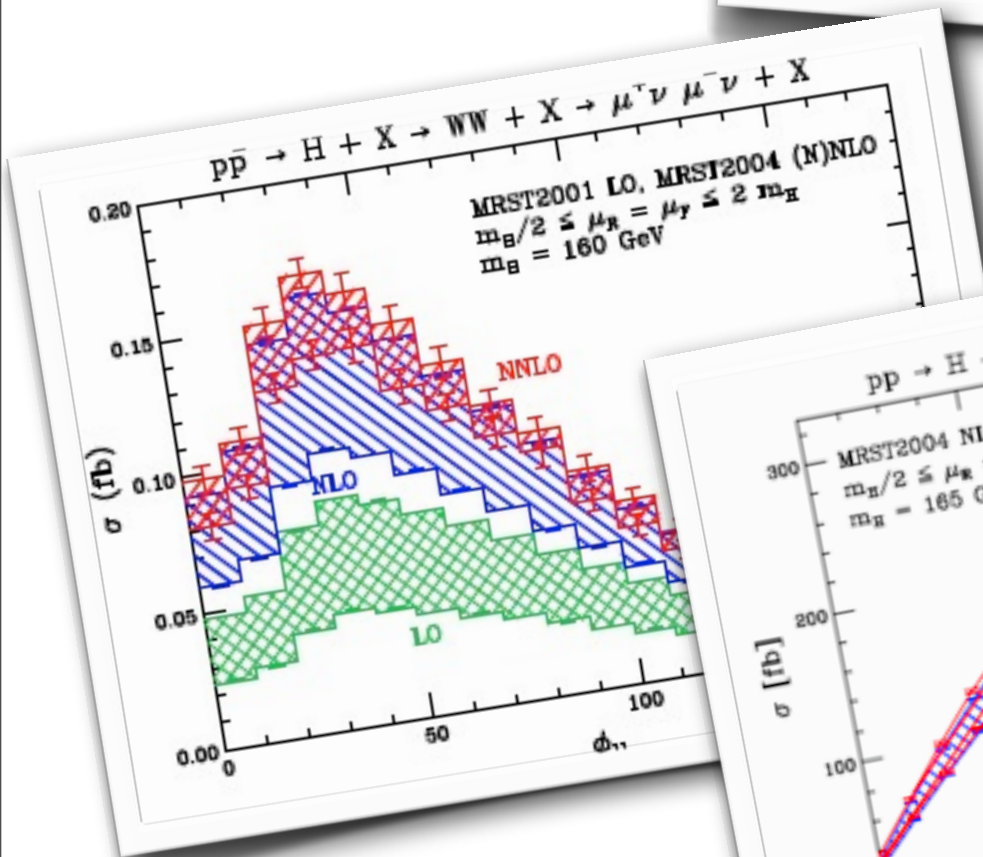
fully differential (Anastasiou, Herzog, AL 2011)

fehip

fully differential ggF (Anastasiou, Melnikov, Petriello 2005)

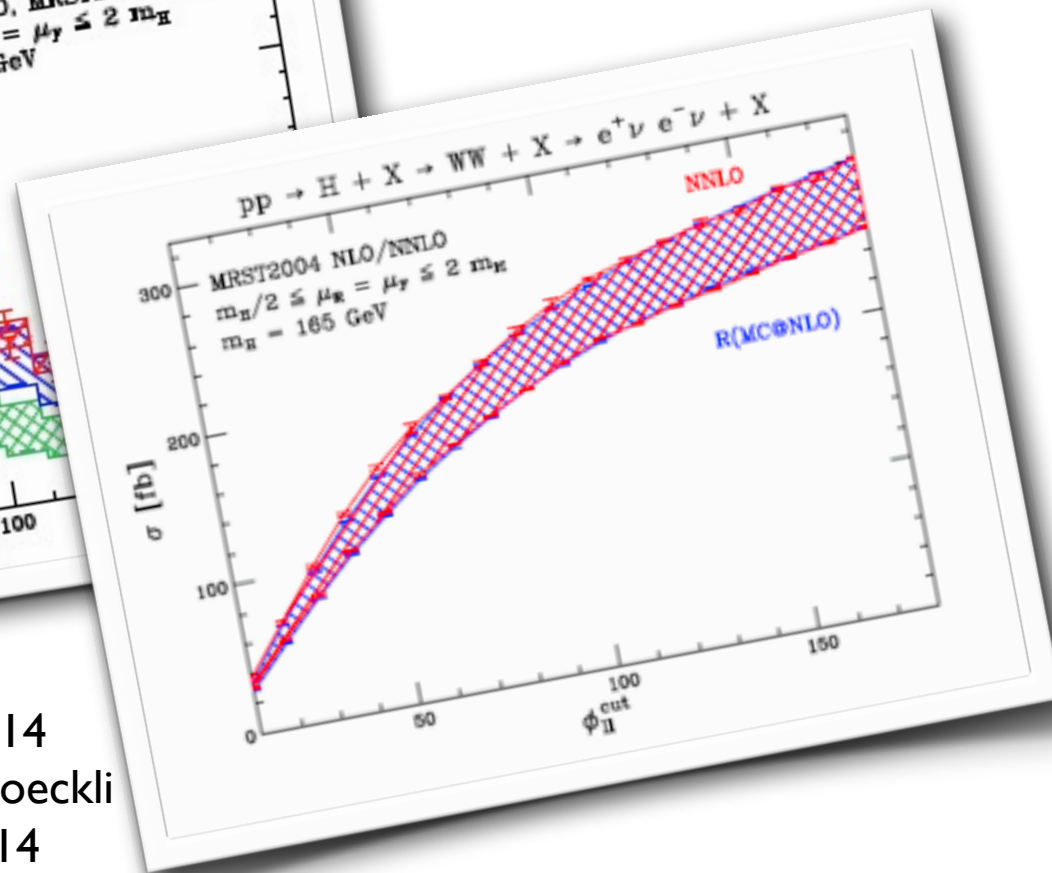


2009, $H \rightarrow WW$, Tevatron
Anastasiou, Dissertori, Grazzini, Stoeckli, Webber



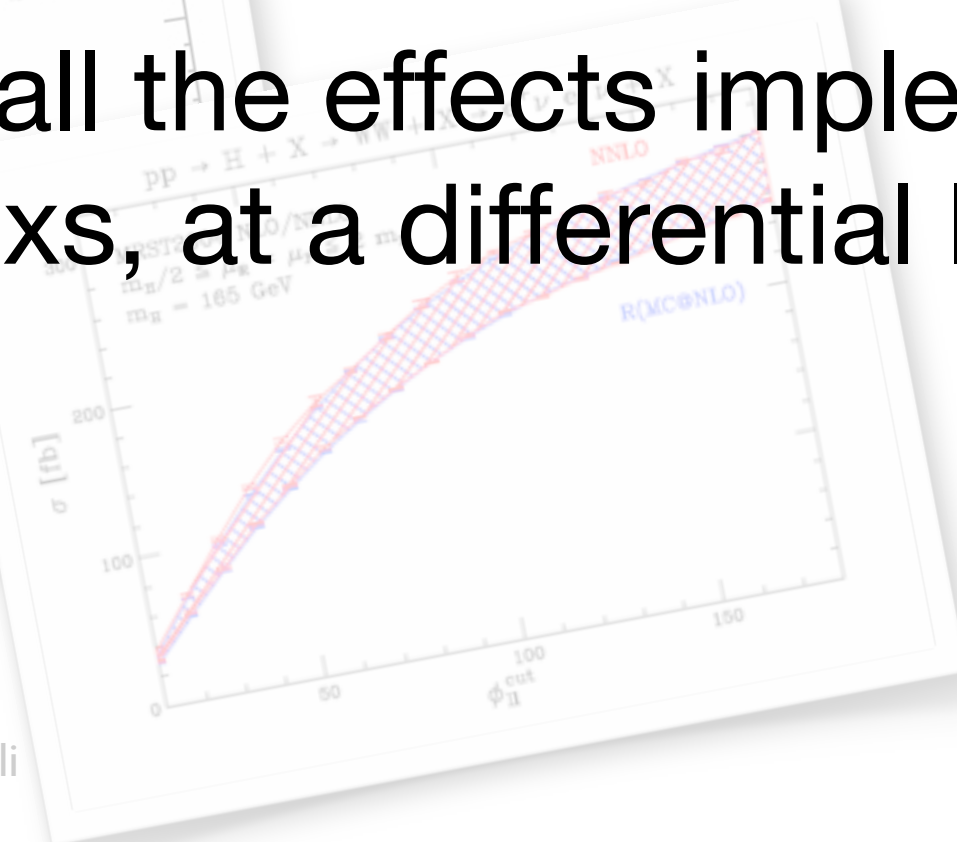
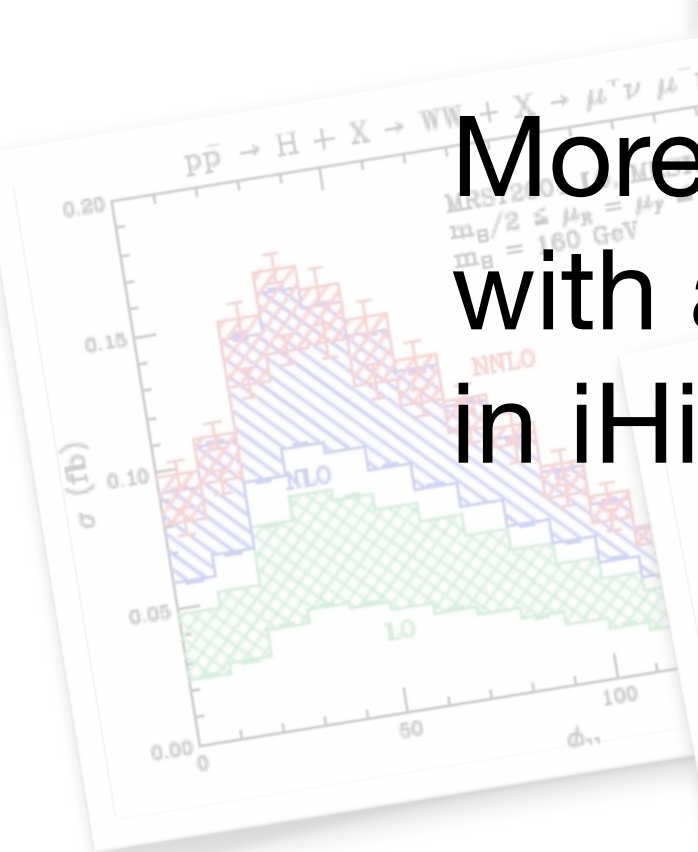
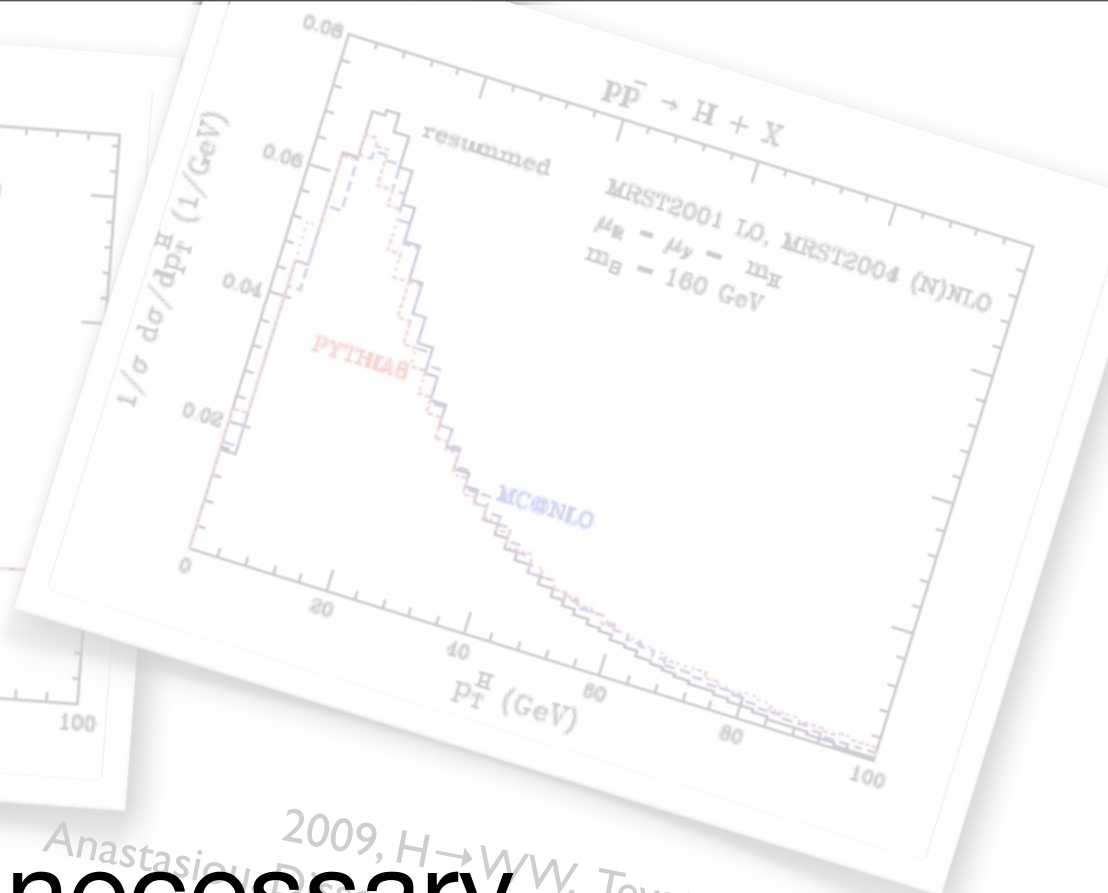
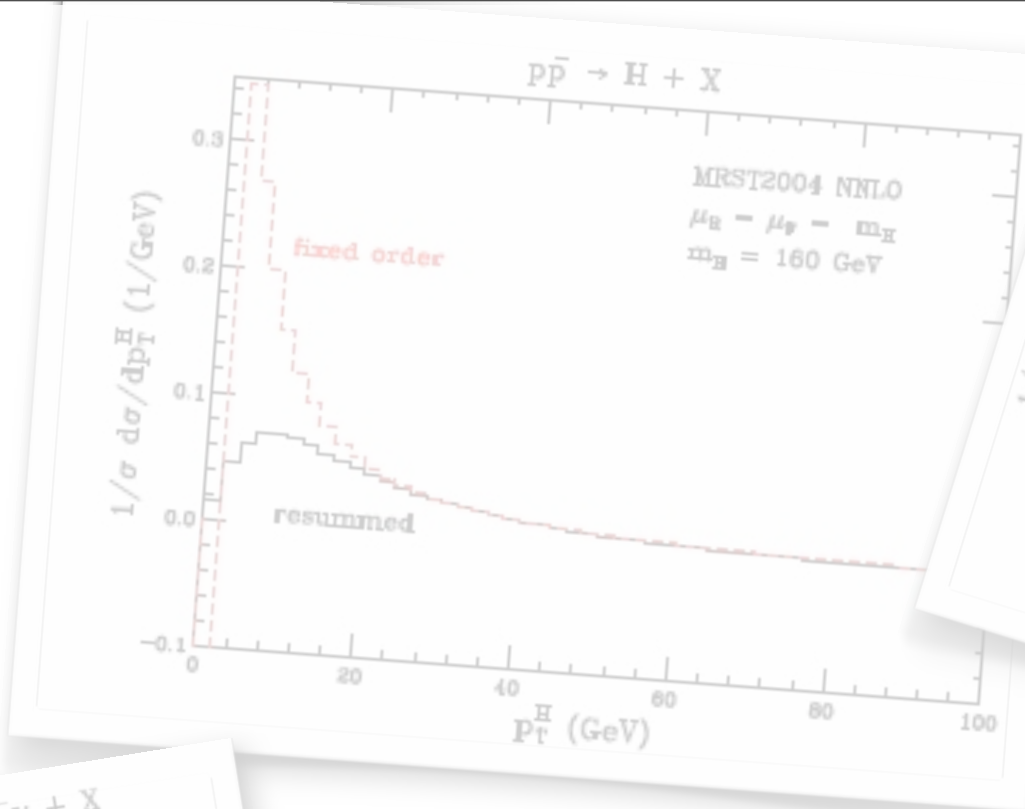
2007, $H \rightarrow WW$ LHC14
Anastasiou, Dissertori, Stoeckli

2008, $H \rightarrow WW$ LHC14
Anastasiou, Dissertori, Stoeckli, Webber



With those tools
important studies on
efficiencies from NNLO
in fully realistic set ups
and comparisons to
MCs have been
achieved

More such studies are necessary,
with all the effects implemented
in iHixs, at a differential level.



2009, $H \rightarrow WW$, Tevatron
Anastasiou, Dissertori, Grazzini, Stoeckli, Webber

2007, $H \rightarrow WW$ LHC14
Anastasiou, Dissertori, Stoeckli
2008, $H \rightarrow WW$ LHC14
Anastasiou, Dissertori, Stoeckli, Webber

Fehipro

Fully differential NNLO,
including exact mass
dependence, EW
effects, ZZ decays etc.



Further improvements (integration of
HPro, python interface, ZZ decay):
Anastasiou, Stoeckli, AL



HPro (2009) (NLO with exact mass
dependence): public (Anastasiou,
Kunszt, Bucherer)

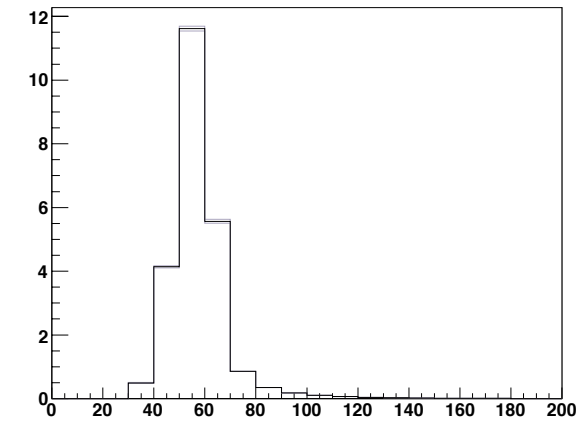


Studies and improvements (ANN, WW
decay) (2007): Anastasiou, Dissertori,
Stoeckli



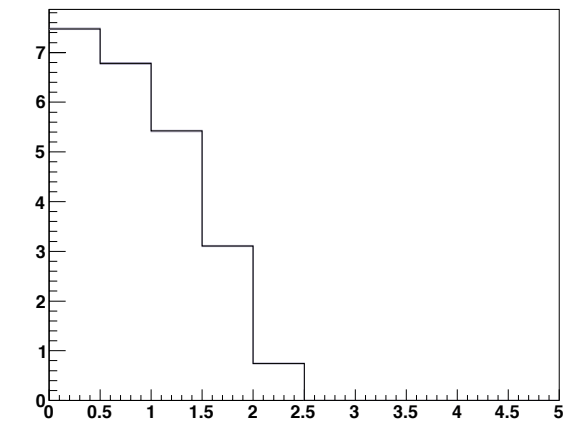
fehpro (2005): public (Anastasiou, Melnikov,
Petriello)

σ (fb) for $m_H=120$



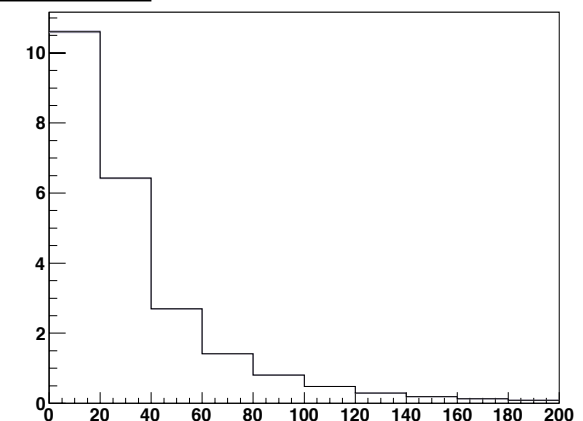
Average p_T of
the photons

σ (fb) for $m_H=120$



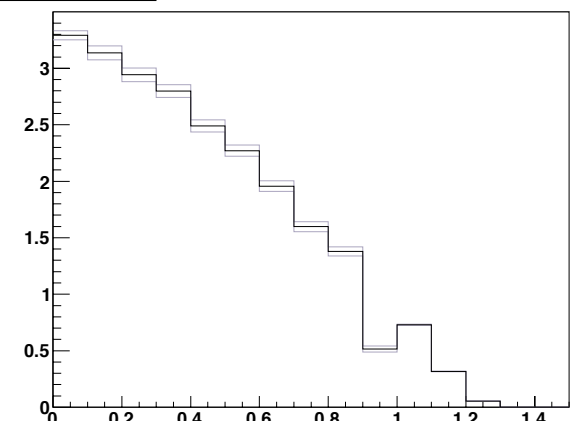
Higgs p_T

σ (fb) for $m_H=120$




Higgs rapidity

σ (fb) for $m_H=120$



Y^*

A large, multi-armed hand, resembling a giant ape or a mythical creature, is shown reaching out from the left side of the frame. The hand is composed of many smaller hands, each with its own fingers spread, creating a complex, branching structure. The background is a solid, light green color. The overall image has a slightly grainy, digital appearance.

**Fehipro is based on
sector decomposition
for the RR**

We would prefer:

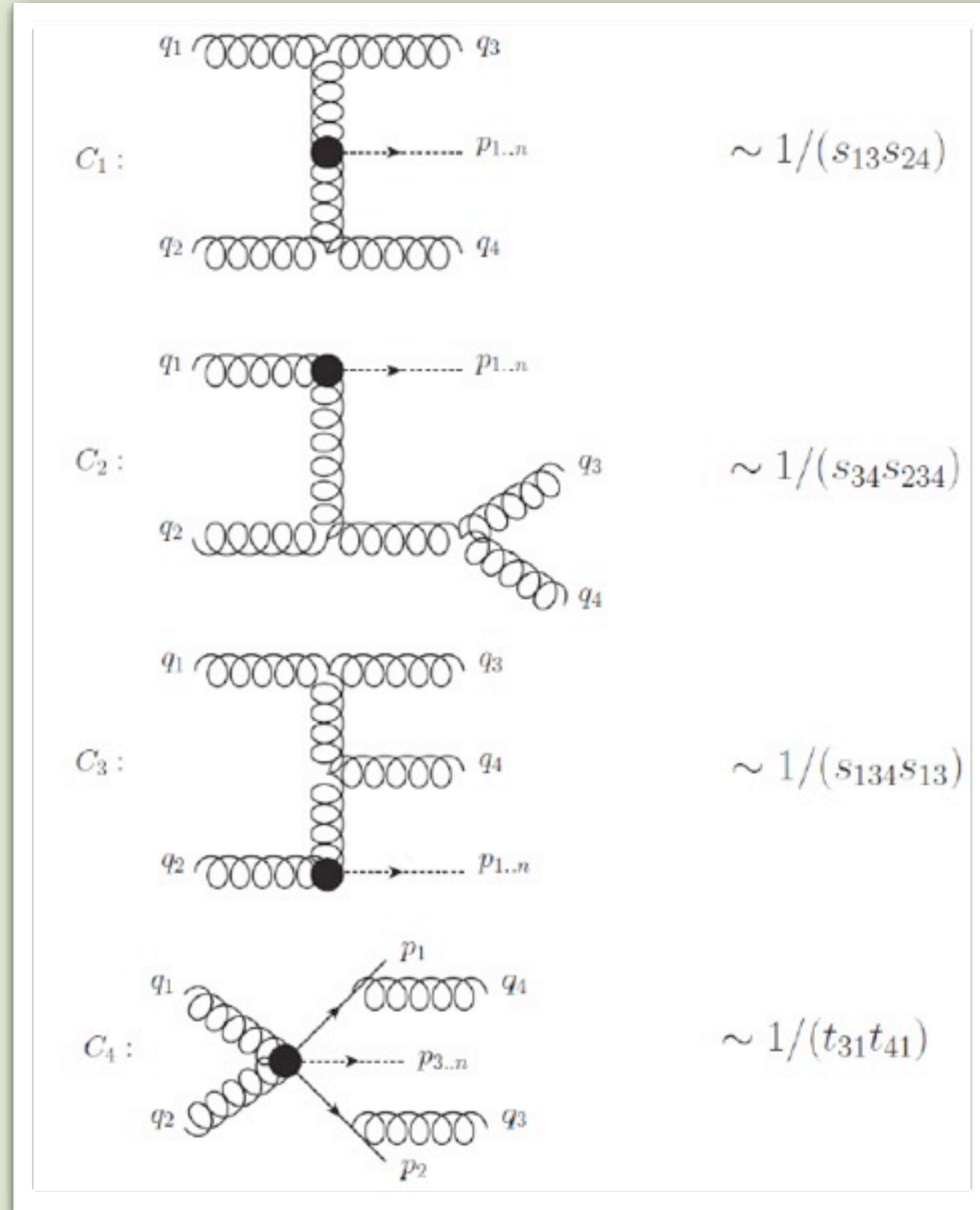
No sectors

Simpler integrals

Universal treatment
of singularities

On the double real (RR)

We catalogue all possible singular kinematic configurations based on denominators of (physical) Feynman diagrams.



On the double real (RR)

Using non-linear mappings we can factorize **all** singularities for **any** singular structure in initial-initial and final-final radiation.

1. Topology $C_1 \otimes C_1$:

$$\int \frac{d\Phi_3 N(\{s_{ij}\})}{(s_{13}s_{24})^2}, \int \frac{d\Phi_3 N(\{s_{ij}\})}{s_{13}s_{23}s_{14}s_{24}}$$

2. Topology $C_2 \otimes C_2$:

$$\int \frac{d\Phi_3 N(\{s_{ij}\})}{(s_{34}s_{134})^2}, \int \frac{d\Phi_3 N(\{s_{ij}\})}{s_{34}^2 s_{134}s_{234}}$$

3. Topology $C_3 \otimes C_3$:

$$\int \frac{d\Phi_3 N(\{s_{ij}\})}{(s_{13}s_{134})^2}, \int \frac{d\Phi_3 N(\{s_{ij}\})}{s_{13}s_{23}s_{134}s_{234}}, \int \frac{d\Phi_3 N(\{s_{ij}\})}{s_{13}s_{24}s_{134}s_{234}}$$

4. Topology $C_1 \otimes C_2$:

$$\int \frac{d\Phi_3 N(\{s_{ij}\})}{s_{34}s_{234}s_{13}s_{24}}$$

5. Topology $C_1 \otimes C_3$:

$$\int \frac{d\Phi_3 N(\{s_{ij}\})}{s_{134}s_{13}s_{23}s_{14}}, \int \frac{d\Phi_3 N(\{s_{ij}\})}{s_{134}s_{13}^2 s_{14}}$$

6. Topology $C_2 \otimes C_3$:

$$\int \frac{d\Phi_3 N(\{s_{ij}\})}{s_{34}s_{134}^2 s_{13}}, \int \frac{d\Phi_3 N(\{s_{ij}\})}{s_{34}s_{134}s_{234}s_{23}}$$

7. Topology $C_4 \otimes C_4$:

$$\int \frac{d\Phi_3 N(\{s_{ij}\})}{t_{i3}^2 t_{j4}^2}, \int \frac{d\Phi_3 N(\{s_{ij}\})}{t_{i3} t_{j4} t_{j3} t_{i4}}$$

8. Topology $C_4 \otimes C_1$:

$$\int \frac{d\Phi_3 N(\{s_{ij}\})}{t_{i3} t_{j4} s_{13} s_{14}}$$

9. Topology $C_4 \otimes C_2$:

$$\int \frac{d\Phi_3 N(\{s_{ij}\})}{t_{i3} t_{j4} s_{34} s_{134}}$$

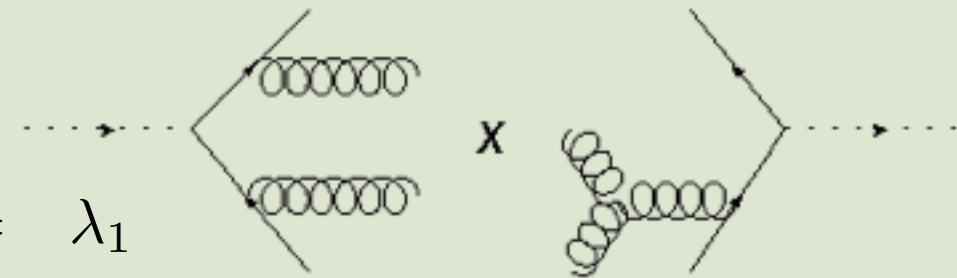
10. Topology $C_4 \otimes C_3$:

$$\int \frac{d\Phi_3 N(\{s_{ij}\})}{t_{i3} t_{j4} s_{13} s_{134}}$$

On the double real (RR)

The singularity structure in each topology is determined by the kinematic invariants that appear in denominators.

We simultaneously factorize them using partial fractioning and **three**, at most, non-linear mappings.



$$\begin{aligned}
 s_{234} &= \lambda_1 \\
 s_{34} &= \lambda_1 \lambda_2 \\
 s_{23} &= \lambda_1 \bar{\lambda}_2 \lambda_4 \\
 s_{24} &= \lambda_1 \bar{\lambda}_2 \bar{\lambda}_4 \\
 s_{12} &= \bar{\lambda}_1 \bar{\lambda}_2 \bar{\lambda}_3 \\
 s_{134} &= \lambda_2 + \lambda_3 \bar{\lambda}_1 \bar{\lambda}_2
 \end{aligned}
 \qquad \bar{\lambda} = 1 - \lambda$$

$$\begin{aligned}
 s_{13} &= \bar{\lambda}_1 \left[\lambda_4 \lambda_3 + \lambda_2 \bar{\lambda}_3 \bar{\lambda}_4 + 2 \cos(\lambda_5 \pi) \sqrt{\lambda_2 \lambda_3 \bar{\lambda}_3 \lambda_4 \bar{\lambda}_4} \right] \\
 s_{14} &= \bar{\lambda}_1 \left[\lambda_3 \bar{\lambda}_4 + \lambda_2 \bar{\lambda}_3 \lambda_4 - 2 \cos(\lambda_5 \pi) \sqrt{\lambda_2 \lambda_3 \bar{\lambda}_3 \lambda_4 \bar{\lambda}_4} \right]
 \end{aligned}$$

$$\begin{aligned}
 \lambda_2 &\mapsto \alpha(\lambda_2, \lambda_3) \\
 \lambda_4 &\mapsto \alpha(\lambda_4, \lambda_2 \bar{\lambda}_3) \\
 \lambda_2 &\mapsto \alpha(\lambda_2, \bar{\lambda}_1)
 \end{aligned}$$

$$\alpha(x, A) := \frac{x A}{x A + \bar{x}}$$

On the double real (RR)

Note that the process-specific numerator can be kept **arbitrary**.

2. Topology $C_2 \otimes C_2$:

$$\int \frac{d\Phi_3 N(\{s_{ij}\})}{(s_{34}s_{134})^2}, \int \frac{d\Phi_3 N(\{s_{ij}\})}{s_{34}^2 s_{134} s_{234}}$$

3. Topology $C_3 \otimes C_3$:

$$\int \frac{d\Phi_3 N(\{s_{ij}\})}{(s_{13}s_{134})^2}, \int \frac{d\Phi_3 N(\{s_{ij}\})}{s_{13}s_{23}s_{134}s_{234}}, \int \frac{d\Phi_3 N(\{s_{ij}\})}{s_{13}s_{24}s_{134}s_{234}}$$

4. Topology $C_1 \otimes C_2$:

$$\int \frac{d\Phi_3 N(\{s_{ij}\})}{s_{34}s_{234}s_{13}s_{24}}$$

5. Topology $C_1 \otimes C_3$:

$$\int \frac{d\Phi_3 N(\{s_{ij}\})}{s_{134}s_{13}s_{23}s_{14}}, \int \frac{d\Phi_3 N(\{s_{ij}\})}{s_{134}s_{13}^2 s_{14}}$$

6. Topology $C_2 \otimes C_3$:

$$\int \frac{d\Phi_3 N(\{s_{ij}\})}{s_{34}s_{134}^2 s_{13}}, \int \frac{d\Phi_3 N(\{s_{ij}\})}{s_{34}s_{134}s_{234}s_{23}}$$

To extend the calculation to a new process we just need to project the new RR matrix elements on the topology basis!

On the double real (RR)

The fully soft limit is special: it exposes universal threshold contributions. We parametrize double soft singularities by a single variable (Q/E) which is never re-mapped.

$$\sigma^{RR} = \tilde{\sigma}_{ij}^{RR}(1) \int dz (1-z)^{-1-4\epsilon} \mathcal{L}_{ij}(z) + \int dz \mathcal{L}_{ij}(z) (1-z)^{-4\epsilon} \left[\frac{\tilde{\sigma}_{ij}^{RR}(z) - \tilde{\sigma}_{ij}^{RR}(1)}{1-z} \right].$$

Threshold contributions: all remaining phase-space variables are integrated once and for all.

Singular in at most three PSP variables. Contains initial state collinear singularities are cancelled numerically against convolutions with splitting functions.

On the Real-Virtual (RV)

Complication: Singular limit from phase space integration of a virtual amplitude.

(Non-smooth off-shell to on-shell limits of master integrals).

The loop amplitude must be cast in a form that exposes the limit smoothly.

Non-linear mappings is a method to do so.

$$\int d\text{PS}_3 \frac{{}_2F_1\left(1, 1 - \epsilon, -\epsilon, -\frac{u}{t}\right)}{ut}$$

$${}_2F_1\left(1, 1 - \epsilon, -\epsilon, -\frac{u}{t}\right) = -\epsilon t \int_0^1 dx_3 \frac{x_3^{-1-\epsilon}}{t + ux_3}$$

$$x_3 \mapsto \frac{x_3 t / u}{1 - x_3 + t / u}$$

On the collinear subtraction

Collinear subtraction terms are non-trivial at NNLO.
Usually treated analytically to supply cancelation terms to the partonic cross sections.

$$\sigma = \int_0^1 dx_1 dx_2 f_i(x_1) f_j(x_2) \overset{\text{DIV}}{\sigma_{ij}}(x_1, x_2)$$

$$f_i(x) = \left(\overset{\text{DIV}}{\Delta_{ij}} \otimes \tilde{f}_j \right) (x)$$

$$\sigma = \int_0^1 dx_1 dx_2 \underset{\text{FIN}}{\tilde{f}_k}(x_1, \mu_f) \underset{\text{FIN}}{\tilde{f}_l}(x_2, \mu_f) \underset{\text{FIN}}{\tilde{\sigma}_{kl}}(x_1, x_2)$$

$$\tilde{\sigma}_{ij}(x_1, x_2) = \int_0^1 dy_1 dy_2 dz_1 dz_2 \delta(y_1 - z_1 x_1) \delta(y_2 - z_2 x_2) \sigma_{kl}(y_1, y_2, \mu_f) \Delta_{ki}(z_1) \Delta_{lj}(z_2) \quad \leftarrow \text{2-d integral over cross-section!}$$

On the collinear subtraction

But if we use the bare PDF's, expanded in strong coupling and the dimensional regulator, we have a **universal** treatment.

Numerical implementation of bare PDFs in a grid, like the renormalized ones.

$$\sigma = \int_0^1 dx_1 dx_2 f_i(x_1) f_j(x_2) \sigma_{ij}(x_1, x_2)$$

$$f_i(x) = \left(\underset{\text{DIV}}{\Delta_{ij}} \otimes \tilde{f}_j \right) (x)$$

$$\Delta_{ij}^{(0)}(z) = \delta_{ij} \delta(1-z),$$

$$\Delta_{ij}^{(1)}(z) = \frac{P_{ij}^0}{\epsilon}$$

$$\Delta_{ij}^{(2)}(z) = \frac{P_{ij}^1(z)}{2\epsilon} + \frac{1}{2\epsilon^2} [(P_{ik}^0 \otimes P_{kj}^0)(z) - \beta_0 P_{ij}^0(z)]$$

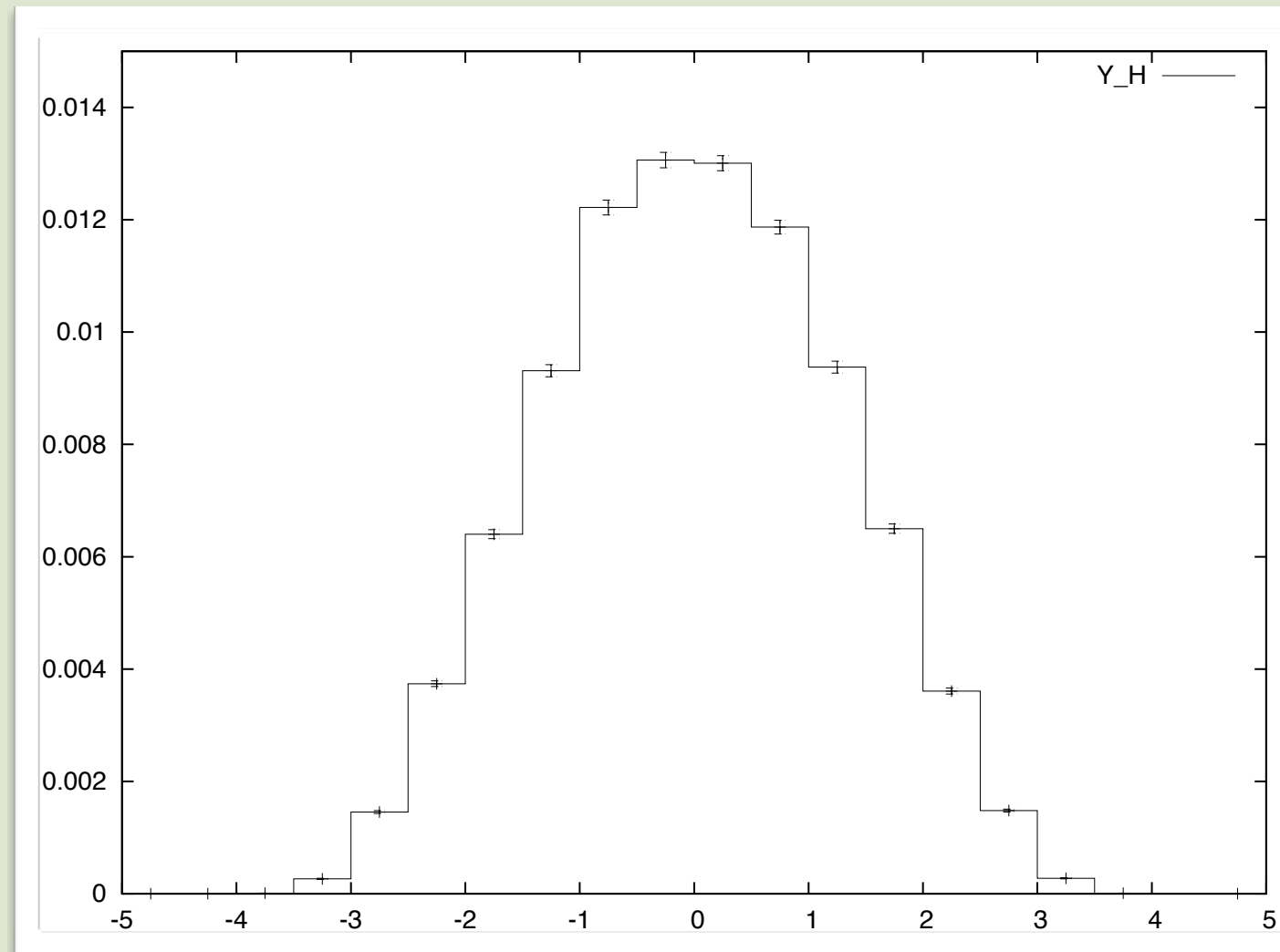
$$f_i(z) = f_i^{(0)}(z) + \left(\frac{\alpha_s(\mu)}{\pi} \right) f_i^{(1)} + \left(\frac{\alpha_s(\mu)}{\pi} \right)^2 f_i^{(2)} + \dots$$

$bb \rightarrow H$ differentially @ NNLO

- Calculation in progress:
 - ✓ Full LO and NLO
 - ✓ Double virtual
 - ✓ Virtual square
 - ✓ Double real implemented
 - ✓ ggbbH sub-channel completed.
 - ★ Real-Virtual in implementation.
- ◎ Two independent numerical implementations of the double real subtraction process.
- $gg \rightarrow H$ also in progress: no extra effort for the Double Real.

$bb \rightarrow H$ differentially @ NNLO

- Very preliminary result: the Higgs rapidity distribution in the $gg \rightarrow bbH$ channel subchannel.
- Applying cuts on the b-quarks, the total rate is checked against MCFM.



Rapidity of H in $gg \rightarrow bbH$ channel

5
integrals

15 mins
on laptop

Conclusions

- Years of work by the theory community have resulted to very accurate predictions for the Higgs signal event rates, inclusively and differentially.
- There is still room for improvement, especially in the high mass region, where the Higgs line-shape affects significantly the exclusion/discovery interpretation. iHixs is a flexible tool that can incorporate any
- A lot remains to be done for fully differential calculations that will be even more important when the (some) Higgs is discovered.
- We see a way to systematize the treatment of the double real emission at NNLO. We apply it to gluon fusion and bbH .
- We are building a framework that is fully generic, and is ready to engage processes with colorful and/or massive final states.